KeAi
CHINESE ROOTS
GLOBAL IMPACT

Available online at www.sciencedirect.com

ScienceDirect

Green Energy & Environment 9 (2024) 1679–1697

www.keaipublishing.com/gee

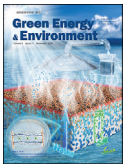

Review Article

CO_2 mineralization by typical industrial solid wastes for preparing ultrafine $CaCO_3$: A review

Run Xu [a,1], Fuxia Zhu [a,1], Liang Zou [a], Shuqing Wang [a], Yanfang Liu [a], Jili Hou [a], Chenghao Li [a], Kuntong Song [a], Lingzhao Kong [b,*], Longpeng Cui [a,*], Zhiqiang Wang [a,*]

[a] Department of Coal and Syngas Conversion, Sinopec Research Institute of Petroleum Processing CO., Ltd., Beijing, 100083, China
[b] School of Environmental Science and Engineering, Suzhou University of Science and Technology, Suzhou, 215000, China

Received 1 May 2024; revised 19 July 2024; accepted 9 August 2024
Available online 13 August 2024

Abstract

Mineral carbonation is a promising CO_2 sequestration strategy that can utilize industrial wastes to convert CO_2 into high-value $CaCO_3$. This review summarizes the advancements in CO_2 mineralization using typical industrial wastes to prepare ultrafine $CaCO_3$. This work surveys the mechanisms of CO_2 mineralization using these wastes and its capacities to synthesize $CaCO_3$, evaluates the effects of carbonation pathways and operating parameters on the preparation of $CaCO_3$, analyzes the current industrial application status and economics of this technology. Due to the large amount of impurities in solid wastes, the purity of $CaCO_3$ prepared by indirect methods is greater than that prepared by direct methods. Crystalline $CaCO_3$ includes three polymorphs. The polymorph of $CaCO_3$ synthesized by carbonation process is determined the combined effects of various factors. These parameters essentially impact the nucleation and growth of $CaCO_3$ by altering the CO_2 supersaturation in the reaction system and the surface energy of $CaCO_3$ grains. Increasing the initial pH of the solution and the CO_2 flow rate favors the formation of vaterite, but calcite is formed under excessively high pH. Vaterite formation is favored at lower temperatures and residence time. With increased temperature and prolonged residence time, it passes through aragonite metastable phase and eventually transforms into calcite. Moreover, polymorph modifiers can decrease the surface energy of $CaCO_3$ grains, facilitating the synthesis of vaterite. However, the large-scale application of this technology still faces many problems, including high costs, high energy consumption, low calcium leaching rate, low carbonation efficiency, and low product yield. Therefore, it is necessary to investigate ways to accelerate carbonation, optimize operating parameters, develop cost-effective agents, and understand the kinetics of $CaCO_3$ nucleation and crystallization to obtain products with specific crystal forms. Furthermore, more studies on life cycle assessment (LCA) should be conducted to fully confirm the feasibility of the developed technologies.

Keywords: Industrial solid wastes; Resource utilization; Mineral carbonation; Ultrafine $CaCO_3$; Carbon emission reduction

1. Introduction

The current global carbon dioxide (CO_2) emissions have surpassed 35 billion tons annually and are projected to double by 2050 [1]. In 2020, CO_2 emissions resulting from the burning of fossil fuels in China amounted to 10 billion tons. Of this total, 47% originated directly from the energy sector, 30% from industry, 11% from transportation, and 3% from construction. The escalating crisis of global warming crisis has dramatically intensified concerns regarding human-caused. In 2018, the Intergovernmental Panel on Climate Change set a target of limiting the global temperature increase to no more than 1.5 °C by the close of this century. Various studies have demonstrated that carbon capture,

* Corresponding authors.
E-mail addresses: lizhkong@usts.edu.cn (L. Kong), lpcui27@163.com (L. Cui), wangzhiqiang.ripp@sinopec.com (Z. Wang).
Peer review under the responsibility of Editorial Board of Green Energy & Environment.
[1] These authors contributed equally to this work.

https://doi.org/10.1016/j.gee.2024.08.002

utilization, and storage (CCUS) can effectively mitigate global warming and address climate change by reducing CO_2 emissions [2]. According to the International Energy Agency, CCUS needs to account for 15% of emissions reduction to reach carbon neutrality by 2070. Mineral carbonation, as one of the CCUS technologies, is a promising approach for CO_2 sequestration. It employs natural ores or industrial waste materials containing alkali metals, such as calcium and magnesium, to convert CO_2 into stable carbonates for permanent sequestration (Fig. 1). Mineral carbonation is a thermodynamically spontaneous process and can yield valuable products such as calcium carbonate ($CaCO_3$) [3].

In recent years, there has been extensive research on the preparation of ultrafine $CaCO_3$ through CO_2 mineralization. Crystalline $CaCO_3$ includes three polymorphs [5]: hexagonal vaterite, orthorhombic aragonite, and rhombohedral calcite, in order of increasing thermodynamic stability (Fig. 2a). These polymorphs exhibit various morphologies, such as cubic, rod-like, spherical, flower-like, chain-like, needle-like, flake-like, and spindle-like structures (Fig. 2b). The diverse range of morphologies and polymorphs of $CaCO_3$ make it an incredibly significant material for both scientific research and technological applications [6–8]. The raw materials used for CO_2 mineralization to synthesize $CaCO_3$ include natural minerals and industrial solid wastes. Natural minerals such as quicklime (CaO), slaked lime ($Ca(OH)_2$), and gypsum ($CaSO_4 \cdot 2H_2O$) require various pretreatments, such as mining, milling, heat treatment, and chemical activation, to enhance their reactivity, which limited the practical application of this technology due to the high energy demands and costs required to achieve sufficient mineralization rates. Compared to natural minerals, industrial wastes offer several advantages for CO_2 mineralization: (1) They are rich in supply, eliminating the need for mining and reducing the costs of raw material extraction and its environmental impact; (2) They are low-cost and often located near CO_2 emission sources, decreasing expenses related to raw materials and transportation; (3) They have smaller particle sizes, which obviates the need for additional crushing and grinding; (4) They exhibit weaker chemical stability than natural minerals, enhancing reaction activity and reducing the energy required for pretreatment and reaction; and (5) they increase the pH of the system when dissolved in water, facilitating CO_2 uptake. Moreover, mineral carbonation significantly decreases the alkalinity of industrial solid waste and converts it into very stable products, reducing environmental hazards. In conclusion, the production of high-value $CaCO_3$ through CO_2 mineralization using industrial solid wastes not only helps mitigate and manage CO_2 emissions but also represents an innovative approach for the large-scale and high-value application of alkaline solid waste.

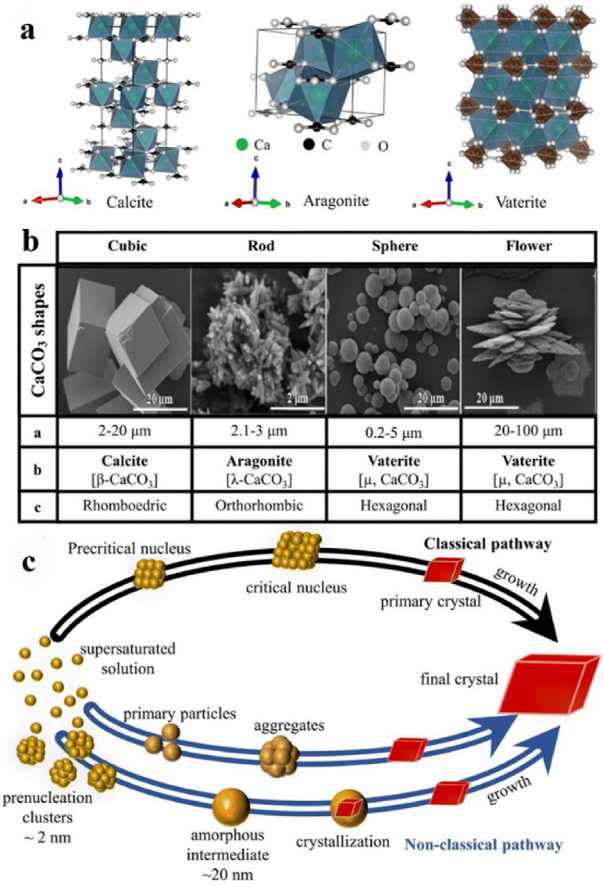

Fig. 2. Structure, size and morphology, and polymorphism of $CaCO_3$ micro/nanoparticles and the associated formation pathways [9]. (a) Polymorphs and crystal structure of $CaCO_3$. (b) Typical shapes of $CaCO_3$ particles. (c) Classical and non-classical pathways to $CaCO_3$.

The preparation of ultrafine $CaCO_3$ through CO_2 mineralization using industrial wastes is a complex process involving multiple chemical reactions. To control the synthesis of $CaCO_3$ and its physical and chemical properties, understanding the nucleation and growth mechanism of the material is

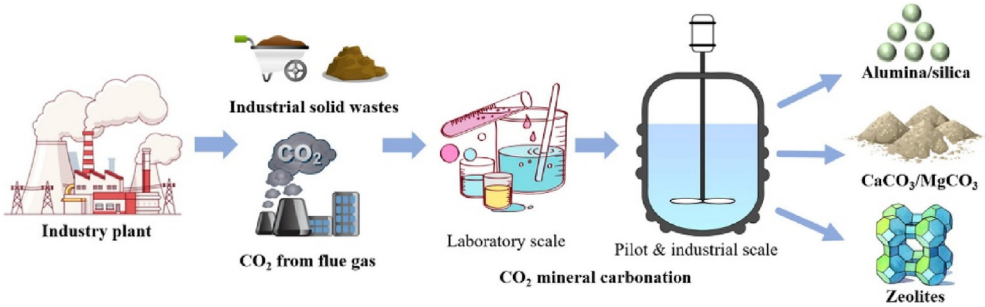

Fig. 1. Schematic diagram of CO_2 mineralization storage technology [4].

essential. The model of $CaCO_3$ nucleation can be seen in Fig. 2c. This process is primarily explained by classical nucleation theory, which assumes a straightforward relationship between Ca^{2+} and CO_3^{2-}, the formation of a supersaturated solution, and the presence of stable nuclei. However, classical nucleation theory fails to account for unexpected nucleation pathways that occur through metastable/stable precursor phases such as prenucleation clusters, amorphous phases, and oligomers. These intermediates may play important roles in the nucleation and subsequent structural control of $CaCO_3$, leading to what is known as the non-classical nucleation pathway (Fig. 2c). Currently, the synthesis of $CaCO_3$ can be controlled by adjusting various operating parameters during the carbonation process. These parameters primarily include the liquid-to-solid ratio, solution pH, CO_2 flow rate, reaction temperature, residence time, and presence of polymorph modifiers [10]. These parameters essentially impact the nucleation and growth of $CaCO_3$ by altering the CO_2 supersaturation in the reaction system and the surface energy of $CaCO_3$ grains [11]. Increasing the initial pH of the solution and the CO_2 flow rate can enhance CO_2 supersaturation, which favors the formation of vaterite [12]. However, excessively high pH promotes the formation of calcite [13]. The reaction temperature affects CO_2 solubility, thereby influencing the contact time between the gas and liquid and the reaction rate of carbonation. Lower reaction temperatures are beneficial for the formation and stability of vaterite, while higher reaction temperatures promote the transformation of vaterite into calcite through a dissolution and recrystallization process [14]. The thermodynamic properties of vaterite are unstable, and vaterite easily converts to calcite in aqueous solution. Therefore, reducing the residence time is advantageous for the formation of vaterite when preparing $CaCO_3$ products in aqueous solutions [14]. Some studies have demonstrated that the addition of polymorph modifiers during carbonation can decrease the surface energy of $CaCO_3$ grains, facilitating the synthesis of vaterite [15–17]. In this process, polymorph modifiers serve two main purposes. First, they alter the interfacial properties of the reaction system by interacting with ions or molecules, reducing the concentration of reaction precursors and thereby lowering the thermodynamic driving force for the nucleation of $CaCO_3$ [15]. Second, polymorph modifiers adsorb onto the unique crystal surface of vaterite, creating steric hindrance that inhibits or delays nucleation of $CaCO_3$ grains or further transforms into stable polymorphs [16]. Common polymorph modifiers include inorganic salts, alcohols, amino acids, and surfactants [5,17]. In addition, some studies have utilized unconventional processes such as ultrasonic methods [18] or microwave-assisted methods [19] to regulate the synthesis of vaterite.

This study provides a review of the advancements in CO_2 mineralization by employing common industrial solid wastes such as steel slag, calcium carbide slag, discarded gypsum, and fly ash for synthesizing ultrafine $CaCO_3$. The potential of these wastes for producing ultrafine $CaCO_3$ was also investigated. This research involved the analysis and comparison of carbonation products obtained from different processes and operating parameters. In addition, the study summarizes the large-scale applications, as well as the environmental and economic benefits, of the most notable technology for $CaCO_3$ synthesis from industrial solid waste. Furthermore, this study assesses the current utilization of industrial wastes in the production of ultrafine $CaCO_3$ and identifies key challenges and issues.

2. Preparation of ultrafine $CaCO_3$ from industrial solid waste

Steel slag, carbide slag, waste gypsum, and fly ash are among the most prevalent industrial solid wastes. Table 1 provides details of the chemical composition of these wastes. Due to their high CaO and MgO contents, these industrial wastes are considered effective materials for CO_2 sequestration. The main methods for mineral carbonation using these wastes can be categorized as direct gas–solid carbonation, direct aqueous carbonation, and indirect carbonation. Among these methods, the direct dry method has low carbonation efficiency. Therefore, this chapter focuses on advancements in synthesizing ultrafine $CaCO_3$ using these four types of industrial solid waste through direct aqueous or indirect carbonation methods.

2.1. Steel slag

The iron and steel industry is recognized for its significant energy consumption and contribution to global CO_2 emissions, accounting for approximately 8% of the annual emissions worldwide [25]. In 2021, the global production of crude steel reached 1951 million tons, with each ton emitting approximately 2 tons of CO_2 and generating 600 kg of steel slag [26,27]. Steel slag consists primarily of basic oxygen furnace slag (BOFS), electric arc furnace slag (EAFS), argon oxygen decarburization slag (AODS), and ladle refining slag (LFS) [28,29]. Its composition typically includes 6–24 wt.% SiO_2, 20–60 wt.% CaO, 1–15 wt.% MgO, and 1.5–10 wt.% Al_2O_3. The utilization of steel slag largely depends on its chemical and mineral content. Currently, approximately 70% of steel slag is used as a building material, such as slag bricks, while approximately 5.5% is utilized as an alternative material for producing green cement [30]. With a pH of approximately 12 and a CaO content exceeding 30%, steel slag is well suited for CO_2 sequestration [31,32]. Furthermore, due to the close proximity of CO_2 and steel slag emission sources in steelmaking, the transportation costs of raw materials are reduced. From the perspective of a circular economy, the use of steel slag as a raw material for synthesizing $CaCO_3$ offers considerable economic value and environmental benefits.

The production of ultrafine $CaCO_3$ through mineral carbonation using steel slag has gained significant attention from researchers. Table 2 provides an overview of the research progress in the synthesis of $CaCO_3$ from steel slag through direct aqueous carbonation and indirect carbonation routes (Fig. 3a). The direct aqueous carbonation process of steel slag involves a three-phase gas–liquid–solid reaction that can be

Table 1
The chemical components of four types of industrial solid wastes.

Types of industrial wastes	CaO (wt.%)	MgO (wt.%)	Al_2O_3 (wt.%)	Fe_2O_3 (wt.%)	SiO_2 (wt.%)	SO_3 (wt.%)	References
Steel slag	20–60	1–15	1.5–10	0.1–1.5	6–24	< 1	[20]
Carbide slag	70–99	1–5	1–5	0.2–1	1–5	< 1	[21,22]
Waste gypgum	28–45	< 1	0.1–1	< 1	0.1–6.5	30–55	[23]
Fly ash	15–35	0–6	5–30	2–10	25–50	1–10	[24]

Table 2
Preparation of $CaCO_3$ by CO_2 mineralization of steel slag under different processes.

Carbonation pathway	Leaching agent	Auxiliary process	Temperature (°C)	Pressure (bar)	Time (min)	Liquid-solid ratio (mL g^{-1})	Ca^{2+} leaching rate (%)	Polymorphs	$CaCO_3$ Yield (g kg^{-1})	References
Direct carbonation	H_2O	/	85	50.0	120	5	/	C	644.3	[22]
	H_2O	/	55	1.5	720	0.18	/	C/A	340.9	[35]
	NaCl	/	150	30.0	/	10	/	C/A	636.4	[36]
	H_2O	/	20	1.0	120	5	/	C/A	290.0	[37]
Indirect carbonation	HCl	Ultrasonic-assisted	20	1.0	120	12.5	/	V	840.0	[41]
	CH_3COOH	/	90–120	6–40	60	7.31	21–24	C/A/V	193–220	[44]
	HCl	/	30	1.0	60	20	73	C	404.7	[46]
	EDTA	/	25	1.0	60	10	/	V	225.0	[50]
	TBP/CH_3COOH	/	94	1.0	60	15	75	/	/	[51]
	NH_4Cl/NH_4NO_3/ CH_3COONH_4	/	Room temperature	1.0	60	50	55	/	489.4	[52]
	NH_4Cl	/	Room temperature	1.0	30	10	50	/	/	[53]
	NH_4Cl	/	80	1.0	60	0.2	60	C/A	/	[54]
	CH_3COOH	/	30	1.0	60	5	25–30	C/A	208.3	[55]
	NH_4Cl	/	60	10	60	10	75	C	527.5	[56]
	NH_4Cl	Microwave-assisted	60	1.0	120	20	40–60	V	/	[57]
	CH_3COOH	/	30	1.0	60	6	82	/	/	[58]

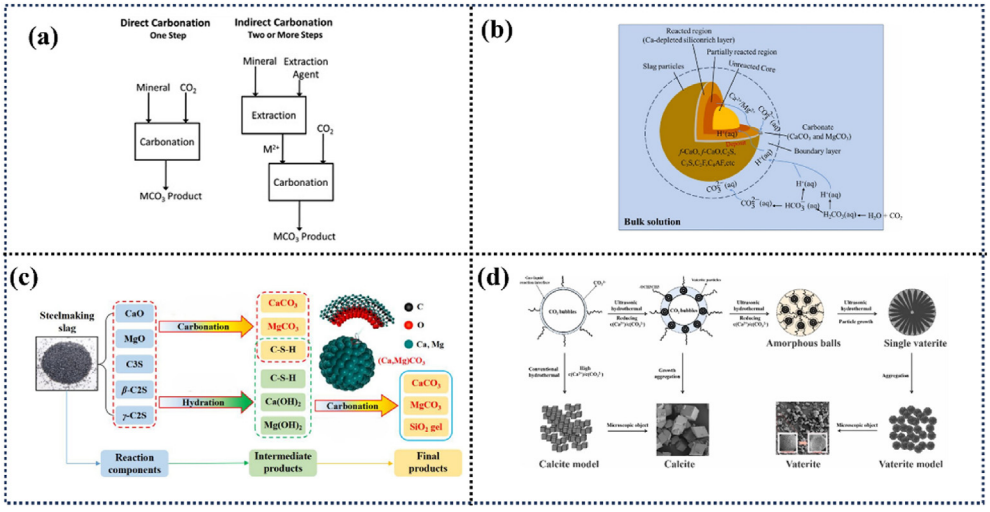

Fig. 3. (a) Direct carbonation process and indirect carbonation process [39]. (b) Schematic diagram of the direct carbonation reaction mechanism based on the shrinking core model [33]. (c) The main hydration and carbonation processes of calcium and magnesium-containing phases in steel-making slag [40]. (d) Mechanistic diagram of the indirect carbonation reaction process [41].

divided into several steps [33]: (1) CO_2 dissolves in water, forming carbonic acid; (2) Carbonic acid ionizes to produce H^+ and HCO_3^-, which further ionizes to H^+ and CO_3^{2-}; (3) Calcium-containing materials within the slag dissolve, and Ca^{2+}/Mg^{2+} ions migrate to the surface of the slag; and (4) these ions react with CO_3^{2-} to form $CaCO_3$/$MgCO_3$. During

direct aqueous carbonation, Young et al. [34] reported that the hydration and carbonation reactions of *f*-CaO/MgO, C_2S, and C_3S in steel slag occur simultaneously. With a lower amount of *f*-CaO/MgO present in the slag, the primary source of Ca^{2+} and Mg^{2+} in aqueous carbonation stems from C_2S and C_3S (Fig. 3c), as shown in equations (1) and (2). As Ca^{2+} is released during the hydration of calcium-containing phases, the remaining silica and impurities form a porous layer on the surface, which, combined with layers of C–S–H gels and $CaCO_3$ products, significantly impedes the diffusion rate of Ca^{2+}.

$$2CaO\cdot SiO_2 + yH_2O + (2-x)CO_2 \rightarrow xCaO\cdot SiO_2\cdot yH_2O + (2-x)CaCO_3 \quad (1)$$

$$3CaO\cdot SiO_2 + yH_2O + (3-x)CO_2 \rightarrow xCaO\cdot SiO_2\cdot yH_2O + (3-x)CaCO_3 \quad (2)$$

Numerous researchers have conducted studies on optimizing the parameters of the carbonation reaction for steel slag to enhance the carbonation efficiency and control the resulting polymorph of $CaCO_3$. Zhu et al. [22] investigated the effect of reaction conditions on the CO_2 sequestration capacity of steel slag and reported that at 85 °C, the CO_2 sequestration capacity reached 283.5 g kg^{-1}, with a carbonation efficiency of 51.61%, and mainly calcite was produced. Conversely, Zhang et al. [35] observed that despite the high CaO content in steel slag, the CO_2 sequestration capacity of 150 g kg^{-1} was relatively low. Ren et al. [36] increased the efficiency of CO_2 mineralization by adding salt solutions (NaCl, $NaNO_3$, CH_3COONa) during carbonation, resulting in a CO_2 sequestration capacity of 280 g kg^{-1} and a mixture of calcite and vaterite. Yi et al. [37] conducted a study on the refining slag and found the carbonation degree reached its maximum value of 39.6% after 120 min of reaction under optimal operating conditions of a temperature of 20 °C, a solid–liquid ratio of 1:5, an aeration rate of 600 mL min and stirring speed of 700 r min^{-1}. Vaterite was generated before 45 min of reaction, while the more stable crystalline calcite and aragonite were generated after 70 min of reaction. The purity of the final carbonation product is 38.34%. The changes in $CaCO_3$ polymorph with increase in carbonation time were consistent with the results of Zhan et al. [38].

Since steel slag contains high amounts of Fe and Al, the purity of $CaCO_3$ produced through direct aqueous carbonation tends to be low. As a result, indirect carbonation methods, which have attracted increasing interest from scholars, are being used to obtain high-purity $CaCO_3$. The indirect carbonation route consists of two steps: extracting Ca/Mg from steel slag under acidic conditions and subsequently undergoing a carbonation reaction under alkaline conditions to produce $CaCO_3$ and $MgCO_3$. The overall efficiency of the carbonation process hinges on the leaching rates of Ca^{2+}/Mg^{2+} during the initial stage. The extraction efficiency of elements in steel slag varies significantly depending on the leaching agents employed. Some leaching agents can extract impurity elements such as Fe, Mn, and Al, while others pose challenges for recovery, leading to new pollution concerns. Hence, the selection of leaching agents and the exploration of leaching process conditions are highly important. Commonly used leaching agents include inorganic acids [42], organic acids [43], and ammonium salts [44]. Additionally, studies have utilized EDTA solution and low-concentration alkaline solution to enhance steel slag leaching and improve carbonation efficiency [45].

Inorganic acids are effective at extracting elements from steel slag, but they also introduce impurity ions such as Fe and Si during the leaching of Ca^{2+}/Mg^{2+}. These impurities decrease the purity of $CaCO_3$. Therefore, alkaline substances are commonly added at the end of the leaching process to remove these impurities and adjust the pH of the solution to levels conducive to carbonation. Taking HCl as an example, the process of extracting Ca^{2+}/Mg^{2+} from steel slag and the carbonation reaction can be described by equations (3) and (4), respectively. Jo et al. [46] and Abhilash et al. [47] used HCl and H_2SO_4, respectively, to leach Ca^{2+}/Mg^{2+} from steel slag. Subsequently, alkalis were introduced to the leachate to adjust the pH to 12.6, facilitating the carbonation reaction, which produced calcite with a purity of 98.5%.

$$Ca_xMg_ySi_zO_{x+y}(s) + 2(x+y)HCl(aq) \rightarrow xCaCl_2(aq) + yMaCl_2(aq) + zSiO_2(s) + (x+y)H_2O(l) \quad (3)$$

$$(Ca,Mg)Cl_2(aq) + CO_2(g) + 2NaOH(l) \rightarrow (Ca,Mg)CO_3(s) + H_2O(l) + 2NaCl(l) \quad (4)$$

Acetic acid is the most commonly used weak organic acid for leaching Ca^{2+}/Mg^{2+} from steel slag. The extraction process and carbonation process can be described by equations (5) and (6), respectively. Notably, equation (6) indicates the potential for acetic acid to be recovered and recycled. The extraction of Ca^{2+}/Mg^{2+} using acetic acid involves the following steps [48]. Initially, the H^+ ions from acetic acid bind to oxygen atoms on the mineral surfaces, weakening the bonds between these atoms and the metal ions. Subsequently, CH_3COO^- complexes with the metal ions, further disrupting the bonds between the cations and oxygen, which enhances dissolution. This complexation also reduces the saturation index of the solution, promoting further dissolution. While acetic acid effectively extracts metal elements, it does not dissolve the silicate framework. Instead, acetic acid undergoes a nucleophilic substitution reaction with silicate minerals, where organic acid anions attack the silicon atoms in the silicon oxygen tetrahedra and replace the oxygen atoms [49]. Chiang et al. [44] believed that acetic acid has selectivity for calcium in steel slag, effectively limiting the leaching of aluminum, which improves the purity of $CaCO_3$ generated during the carbonation process. Mun et al. [50] reported that when water and 0.1% EDTA solution were used as leaching agents, the Ca^{2+} concentrations in the leachate were 66.60 mg L^{-1} and 1949 mg L^{-1}, respectively, indicating that

EDTA can improve the leaching performance of Ca^{2+}. The purity of vaterite obtained during the subsequent carbonation process was 79.03%. Furthermore, Bao et al. [51] reported that adding tributyl phosphate (TBP) to a reaction system can also improve the leaching rate of Ca^{2+} when acetic acid is used as a leaching agent.

$$Ca_xMg_ySi_zO_{x+y}(s) + 2(x+y)CH_3COOH(aq) \rightarrow xCa(CH_3COO)_2(aq) + yMg(CH_3COO)_2(aq) + zSiO_2(s) + (x+y)H_2O(l) \quad (5)$$

$$(Ca,Mg)(CH_3COO)_2(aq) + CO_2(g) + 2H_2O(l) \rightarrow (Ca,Mg)CO_3(s) + 2CH_3COOH(l) \quad (6)$$

capability to extract Ca^{2+} from the calcium-containing phase of steel slag but also requires selectivity toward Ca^{2+} to obtain high-purity $CaCO_3$ during the carbonation process. When utilizing ammonium salt as a leaching agent, it appears that only calcium is leached from the steel slag, while the concentrations of other elements are either significantly low or undetectable [52]. In a study conducted by Owais et al. [53], the leaching behavior of Ca^{2+} in steel slag was examined in NH_4Cl solutions of varying concentrations. The findings demonstrated that as the concentration of the NH_4Cl solution increased, so did the leaching rate of Ca^{2+}; however, there were also greater amounts of impurity ions present in the leachate. Kodama et al. [54] investigated the changes in solution pH during the extraction and carbonation processes. The NH_4Cl aqueous solution is acidic, and throughout the extraction process, the pH of the solution transitions from 4.6 to 9.4, subsequently decreasing to 7.26 during carbonation. These pH changes can be explained by equations (7) and (8). As depicted in the equations, it becomes evident that the leaching solution utilized for Ca^{2+} extraction is regenerated after carbonation, thus offering the potential for recycling and reuse. The recovery of leaching agents holds significant economic value. Additionally, the NH_4Cl solution displays a remarkable selectivity for calcium, yielding a calcium conversion rate of 60%. Eloneva et al. [55] compared the leaching performances of NH_4NO_3, CH_3COONH_4, and NH_4Cl for Ca^{2+}. They found that NH_4NO_3 exhibited superior leaching performance, with a calcium ion leaching rate approximately 10% higher than that of CH_3COONH_4 and NH_4Cl.

$$2CaO\cdot SiO_2 + 4NH_4Cl = 2CaCl_2 + 4NH_3 + 2H_2O + SiO_2 \quad (7)$$

$$2CaCl_2 + 4NH_3 + 2CO_2 + 4H_2O = 4NH_4Cl + 2CaCO_3 \quad (8)$$

In summary, the use of various types of acids and ammonium salts as leaching agents in the indirect carbonation process of steel slag has advantages and disadvantages. Strong acids have high corrosiveness and can efficiently extract calcium, but they also introduce impurity ions into the leachate. Acetic acid, while having weak acidity, exhibits high selectivity toward Ca^{2+}. It can effectively extract most of the calcium from steel slag and has lower selectivity for other elements. However, acetic acid also requires the addition of alkaline substances to adjust its pH before carbonation, which hinders its recovery and increases costs. On the other hand, ammonium chloride has a greater leaching rate for calcium and greater selectivity for calcium than strong and weak acids. One of its key advantages is that it does not require the addition of alkaline substances to adjust the pH of the leaching solution. Furthermore, ammonium chloride can be regenerated after carbonization, making it a cost-effective and sustainable leaching agent in the indirect carbonation process of steel slag. Eloneva et al. [52] successfully utilized ammonium salt solution as a leaching agent to extract calcium from steel slag and subsequently produced $CaCO_3$ by bubbling CO_2 into the leaching solution. Sun et al. [56] also achieved impressive results, obtaining a CO_2 sequestration capacity of 211 g kg^{-1} for steel slag and producing $CaCO_3$ with a purity of 96 ± 2% using ammonium salt solution as the leaching agent.

In addition, some researchers have employed auxiliary processes to enhance the leaching rate of Ca^{2+} and the purity of $CaCO_3$. Tong et al. [57] discovered that microwave radiation can increase the leaching rate of Ca^{2+} to 95% and inhibit vaterite transformation to calcite. Similarly, Liu et al. [41] reported that ultrasonic bubbling carbonation is a highly effective method for producing high-purity vaterite from BFS. Through a series of reactions, such as Ca^{2+} leaching, impurity removal, and carbonation under ultrasonic conditions, they successfully prepared uniform vaterite with a purity of approximately 95%. The mechanism underlying this process involves the formation of radiating fibers extending outward from the center of a sphere. As the number of fibers increases, the morphology of $CaCO_3$ shifts to a ball-dumbbell-ball structure, ultimately resulting in the formation of uniform vaterite (Fig. 3d).

Steel slag undergoes high-temperature sintering during its formation process, resulting in the active CaO component typically being located in the crystal structure or encapsulated by silicates or sulfates. This leads to poor reactivity and stability. Therefore, effectively stripping the inert and active components of steel slag, eliminating its instability, and balancing the stripping rate of mineralized active components with the carbonation reaction rate are crucial for producing high value-added $CaCO_3$ products.

2.2. Carbide slag

Carbide slag is an industrial byproduct that is rich in calcium and is generated during the production of acetylene gas. Approximately 1.2–1.8 tons of carbide slag are produced for every 1 ton of acetylene. Currently, China produces approximately 40 million tons of carbide slag annually, with a cumulative stockpile of over 100 million tons [59,60]. Carbide slag is predominantly stored outdoors or disposed of through landfills. This not only occupies a significant amount of land resources but also poses a threat of serious pollution to the soil, atmosphere, and groundwater.

The current methods of resource utilization for carbide slag primarily include the production of building materials such as roadbeds, cement, and concrete, as well as the production of chemical products such as calcium silicate and epichlorohydrin. These methods provide practical and feasible methods for reducing carbide slag. However, there is a need to explore other key technologies that can consume carbide slag on a large scale and produce high value-added products, consequently improving its resource utilization rate and added value. Carbide slag possesses a high $Ca(OH)_2$ content (> 80%), strong alkalinity (pH > 13), fine particles, and a large specific surface area. The production of $CaCO_3$ through CO_2 mineralization using carbide slag not only reduces carbon emissions but also yields high value-added products. In the context of dual carbon targets, the development of this technology holds significant practical significance.

Table 3 presents a summary of the research progress on synthesizing $CaCO_3$ from carbide slag under different process conditions. Many studies have investigated CO_2 sequestration through mineral carbonation of carbide slag, although fewer studies have focused on producing ultrafine $CaCO_3$. In the direct route, Song et al. [61] synthesized vaterite with a content of more than 95% using carbide slag in NH_4Cl, CH_3COONH_4, and $(NH_4)_2S_2O_8$ systems. Fig. 4a depicts the possible formation process of vaterite under the various ammonium systems. Researchers have discovered that NH_4^+ enhances the leaching rate of Ca^{2+}, CH_3COO^- adsorbs to the vaterite surface, and $S_2O_8^{2-}$ induces the appearance of $CaSO_4$ as an intermediate during the reaction. The synergistic interactions among NH_4^+, CH_3COO^-, and $S_2O_8^{2-}$ facilitate the nucleation and growth of vaterite. For the indirect route, the preparation of $CaCO_3$ involves two steps: solution leaching and a carbonation reaction (Fig. 4b). Yao et al. [62] used NH_4Cl to leach Ca^{2+} from carbide slag and thoroughly studied the impact of the CO_2 flow rate, reaction temperature, ammonia dosage, reaction time, and carbonation filtrate cycle index on the crystal phase, grain size, and morphology of the resulting $CaCO_3$. They found that under optimal conditions, spherical vaterite could meet the relevant standards of precipitated $CaCO_3$ for industrial use. Ding et al. [63] also employed NH_4Cl as a leaching agent and successfully synthesized high-purity nanoscale $CaCO_3$ in various crystal forms by controlling the reaction conditions, with vaterite purity and whiteness reaching 99.95% and 99.3%, respectively. Li et al. [21] extracted Ca from carbide slag into $CaSO_4 \cdot 2H_2O$ using a $(NH_4)_2SO_4$ solution and then underwent a "dropwise carbonation" process to produce ultrafine vaterite at 25 °C and 0.1 MPa. The reaction pathway for this process is illustrated in Fig. 4c. Apart from the gas–liquid–solid reaction pathways, Guo et al. [64] proposed a method to synthesize pure vaterite using a saturated limpid solution of carbide slag and a novel CO_2 storage material (CO_2SM) via a hydrothermal homogeneous reaction (Fig. 4d). Furthermore, there have been studies on the preparation of calcite or aragonite through mineral carbonation of carbide slag [62,65–69]. For instance, Ma et al. [67] synthesized spindle-like calcite with controllable sizes using CO_2 (8% CO_2/N_2 mixture gas) and carbide slag as raw

Table 3
Preparation of $CaCO_3$ by CO_2 mineralization of carbide slag under different processes.

Carbonation pathway	Leaching agent	Polymorph modifier	Temperature (°C)	Pressure (bar)	Time (min)	Liquid-solid ratio (mL g^{-1})	Ca^{2+} leaching rate (%)	Polymorphs	$CaCO_3$ Yield (g kg^{-1})	References
Direct carbonation	NH_4Cl	NH_4Cl	Room temperature	1.0	50	/	/	V	/	[61]
	CH_3COONH_4	CH_3COONH_4	Room temperature	1.0	40	/	/	V	/	[61]
	$(NH_4)_2S_2O_8$	$(NH_4)_2S_2O_8$	Room temperature	1.0	30	/	/	V	/	[61]
	Sodium oleate	/	80	1.0	92	50	/	C	/	[68]
	H_2O	/	25	1.0	/	5	/	C	/	[69]
	H_2O	/	65	150	120	15	/	C	1388.2	[79]
	$NH_3 \cdot H_2O$	$NH_3 \cdot H_2O$	20	1.0	60	/	/	V	/	[80]
	Monoethanolamine	Monoethanolamine								
	Triethylamine	Triethylamine	20	1.0	60	/	/	V	/	[80]
	Triethanolamine	Triethanolamine								
	H_2O	/	Room temperature	1.0	10	30	/	C	486.5	[81]
Indirect carbonation	$(NH_4)_2SO_4$	Glycerol, sodium tripolyphosphate	25	1.0	30	6.67	95.3	V	1150.0	[21]
	NH_4Cl	/	25	1.0	60	8	> 10	V/C	/	[62]
	1,2-ethylenediamine	1,2-ethylenediamine	100	/	90	10	/	V	612.6	[64]
	1,2-ethylene glycol	1,2-ethylene glycol								
	NH_4Cl	/	30	1.0	50	10	89–91	C	763.3	[65]
	Trisodium citrate	Trisodium citrate	Room temperature	1.0	30	50	90	C	/	[66]

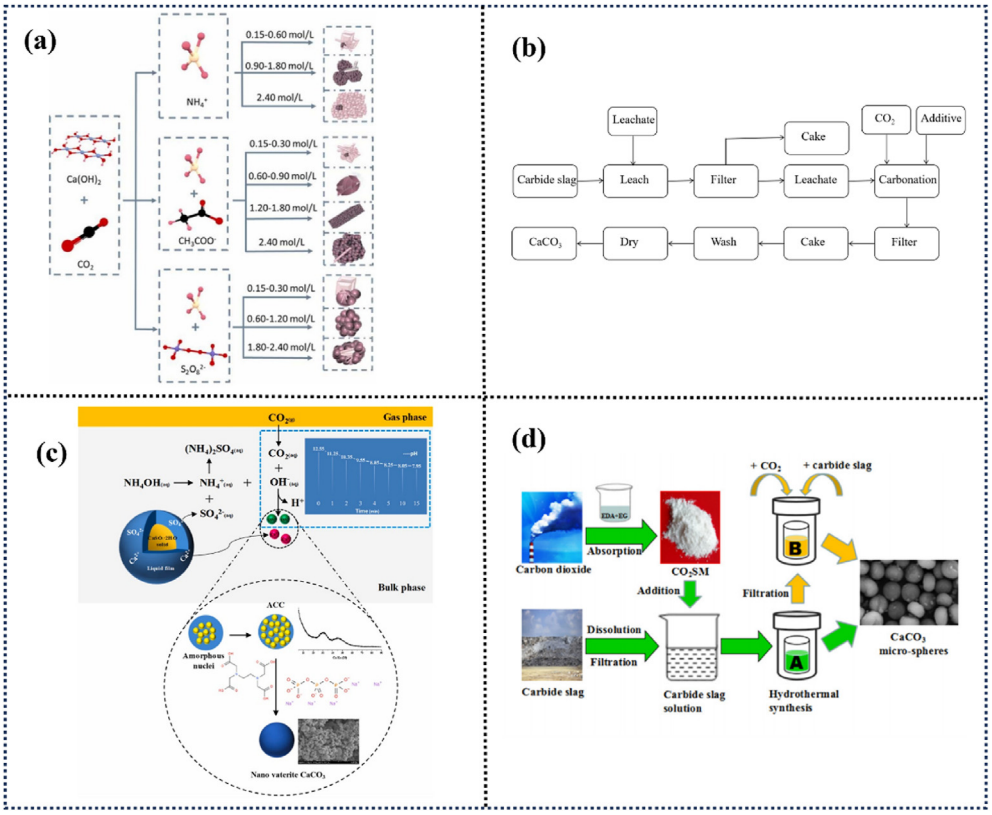

Fig. 4. (a) Direct carbonation mechanism of calcium carbide slag [61]. (b) Indirect aqueous carbonation route for carbide slag [62]. (c) Mechanism of indirect carbonation of carbide slag [21]. (d) Morphology control in the synthesis of $CaCO_3$ microspheres by using carbide slag and CO_2SM, which was prepared from the equimolar system EDA + EG absorbing CO_2 [64].

materials through the atomization method at room temperature. Mahmut [68] prepared calcite by adding sodium oleate to a mineral carbonation system with carbide slag. Mao et al. [69] also converted carbide slag into calcite with particle sizes ranging from 50 to 200 nm under specific reaction conditions, including a calcium hydroxide saturation of 1, a flow rate of 1.5 L min^{-1}, a CO_2 flow rate of 50 mL min^{-1}, and a sodium dodecyl sulfate amount of 2%.

Due to the presence of impurities, the purity of $CaCO_3$ prepared via the direct carbonation of carbide slag is not optimal. However, by implementing the indirect carbonation pathway, the extraction process of a leaching agent can effectively separate Ca^{2+} from solid impurities such as Fe, Si, and Al found in carbide slag. This ultimately yields $CaCO_3$ with enhanced purity and high whiteness. The solution leaching process includes several influencing factors, including the choice of leaching agent and various process parameters, such as temperature, pH, and stirring speed. Leaching agents such as glycine, citric acid, and ammonium salts can all be employed [66,70–72]. Glycine facilitates the leaching of Ca^{2+} during the extraction process, aids in the absorption of carbon dioxide during carbonate precipitation, and functions as a polymorph modifier during crystal growth [72]. The citrate ions present in citrate salts coordinate with Ca^{2+} ions, significantly improving the leaching rate of calcium. This inhibits crystal growth and promotes the formation of nanosized $CaCO_3$ particles during the crystallization process. Ammonium salt solutions such as NH_4Cl and NH_4HSO_4 exhibit high Ca^{2+} leaching rates and are regarded as common and effective leaching agents with considerable potential for development. The production of $CaCO_3$ occurs during the carbonation stage, allowing for the control of process parameters such as Ca^{2+} concentration, temperature, pH, and polymorph modifiers to yield various polymorphs with distinct morphologies and particle sizes. The influence of Ca^{2+} concentration on the reaction system varies; an excessive amount of Ca^{2+} slows the particle formation process and promotes the growth of $CaCO_3$ particles. Conversely, when the Ca^{2+} concentration is low and CO_3^{2-} is plentiful, it accelerates the early nucleation of $CaCO_3$ [73]. Temperature affects both the nucleation and growth rate of $CaCO_3$. Moreover, the solubility of $CaCO_3$ in water changes with temperature, thereby determining the morphology and size of the resulting $CaCO_3$. The pH affects the equilibrium of ions within an aqueous solution. By analyzing the concentration and reactivity of all ions in the solution, one can estimate the supersaturation state of the system, thereby inferring the polymorph of $CaCO_3$. Polymorph modifiers significantly impact the polymorph and morphology of $CaCO_3$. They primarily influence the crystal growth process through three mechanisms: incorporation into the crystal interior, adsorption onto the crystal surface, and alteration of the crystal surface energy, enabling the controlled

preparation of $CaCO_3$ [61]. Common polymorph modifiers include acids, sugars, surfactants, alcohols, and inorganic salts. Organic acids containing carboxyl groups can strongly adsorb with $CaCO_3$ during crystal growth, hindering the further generation of $CaCO_3$ particles and affecting the morphology and particle size of the crystals [74]. Inorganic acids primarily influence the formation of $CaCO_3$ via chemical reactions. For example, H_3PO_4 rapidly reacts with Ca^{2+} to form needle-shaped hydroxyapatite (HAP). During the carbonation process, HAP acts as a heterogeneous nucleating agent, which supports the formation of aragonite [75]. Sucrose and glucose, both sugar modifiers containing hydroxyl groups, facilitate charge matching with Ca^{2+}, reducing the activation energy of the $CaCO_3$ nucleation process and promoting nucleation while inhibiting crystal growth. However, the carbonation products resulting from the addition of sugar modifiers are primarily calcite. Specific surfactants can selectively bind to distinct crystal faces and offer significant advantages in the controlled preparation of $CaCO_3$, usually leading to the formation of calcite. Alcohol modifiers decrease the solubility of $CaCO_3$, and the interactions between Ca^{2+} and alcohols are weak. This is conducive to the formation of vaterite [76]. During the formation of $CaCO_3$, the introduction of ammonium salts enhances the CO_2 supersaturation of the reaction system. This, in turn, promotes the nucleation of $CaCO_3$ by providing an alkaline environment, favoring the synthesis of metastable vaterite. Additionally, NH_4^+ can form formate salts during the absorption of carbon dioxide, stabilizing vaterite particles [77,78].

In the context of green and sustainable development, the utilization of carbide slag to produce ultrafine $CaCO_3$ offers many advantages. Not only does it help to address the environmental issues caused by the accumulation of solid waste, but it also generates high-value products. This technological approach has significant social and economic benefits. However, the presence of impurities such as residual carbon, Fe_2O_3, Al_2O_3, and MgO in carbide slag poses a significant challenge to its high-value utilization. The traditional method of removing residual carbon through calcination is energy intensive. Furthermore, the use of leaching solutions and additives increases production costs, even though they may result in higher-purity products through an indirect pathway. Therefore, a suitable pretreatment process for impurities in carbide slag, along with the selection of cost-effective and efficient auxiliary agents, is critical for reducing the production costs of ultrafine $CaCO_3$ and achieving large-scale industrialized production.

2.3. Waste gypsum

Waste gypsum can be classified into three categories: flue gas desulfurization gypsum (FGDG), phosphogypsum (PG), and titanium gypsum (TG). FGDG is a solid industrial waste that is produced during the lime-limestone flue gas desulfurization process. Its annual production is approximately 75 million tons, with a $CaSO_4 \cdot 2H_2O$ content as high as 95%. PG is a solid waste generated during the wet process of phosphoric acid production, with an annual output of 160 million tons. The $CaSO_4 \cdot 2H_2O$ content in PG is greater than 90%. TG is a solid waste generated during the production of titanium dioxide using the sulfuric acid method through the neutralization of acidic wastewater with lime. Its main components are $CaSO_4 \cdot 2H_2O$ (> 75%) and Fe_2O_3, with an annual output close to 18.5 million tons.

Waste gypsum is mainly composed of $CaSO_4 \cdot 2H_2O$, which exhibits strong carbonation activity at room temperature and atmospheric pressure. Theoretically, 1 ton of $CaSO_4 \cdot 2H_2O$ could be used, and 1 ton of $CaCO_3$ could be produced by absorbing 0.26 tons of CO_2 [82]. Therefore, waste gypsum has great potential for CO_2 capture and $CaCO_3$ synthesis. The direct carbonation process involves the mineralization of CO_2, waste gypsum, and alkaline substances such as $NH_3 \cdot H_2O$ or NaOH in a reactor. The direct aqueous carbonation of FGDG in an ammonia-mediated system is illustrated in Fig. 5a. Initially, a suspension of FGDG and $NH_3 \cdot H_2O$ was prepared in the slurry tank. Then, the prepared suspension was added to the reactor, and CO_2 was introduced for the mineralization reaction. After the reaction is complete, solid−liquid separation is carried out, resulting in $CaCO_3$ as the solid product. The liquid phase enters the crystallizer, and the reaction system undergoes solid−liquid separation after crystallization to obtain a relatively pure $(NH_4)_2SO_4$ product. The mother liquor is returned to the crystallizer for reuse. In addition, volatile ammonia is recovered through an ammonia recovery tank, and the recovered ammonia is further used to prepare suspensions of FGDG and $NH_3 \cdot H_2O$. The entire process can be described using the following equation:

$$CaSO_4 \cdot 2H_2O(s) + CO_2(g) + 2NH_4OH(aq) \rightarrow (NH_4)_2SO_4(aq) + CaCO_3(s) + 3H_2O$$

In addition to $NH_3 \cdot H_2O$, NaOH and organic bases are also used as alkaline media for the direct aqueous carbonation of FGDG [83]. Tan et al. [84] evaluated the effects of three different alkaline media, namely $NH_3 \cdot H_2O$, triethanolamine (TEA), and hexamethylenetetramine (HMT), on the conversion of FGDG at different temperatures.

The results indicate that in the alkaline system of $NH_3 \cdot H_2O$, FGDG was not completely converted into $CaCO_3$ at 60 °C and 80 °C due to the volatilization of $NH_3 \cdot H_2O$. However, in the alkaline systems of TEA and HMT, the conversion rate of FGDG exceeded 95% even at 80 °C, demonstrating that these organic bases effectively overcome the volatilization problem of $NH_3 \cdot H_2O$ at high temperatures. Like inorganic bases, organic bases react with CO_2 during carbonation to form CO_3^{2-}, which then react with Ca^{2+} from FGDG to produce $CaCO_3$. Despite the potential for $NH_3 \cdot H_2O$ loss at temperatures above 60 °C, it remains an attractive option for FGDG mineralization due to the well-established ammonia synthesis technology and the affordability of $NH_3 \cdot H_2O$.

Numerous scholars have conducted research on the synthesis of $CaCO_3$ using waste gypsum through direct aqueous carbonation (Table 4). Various factors influence the

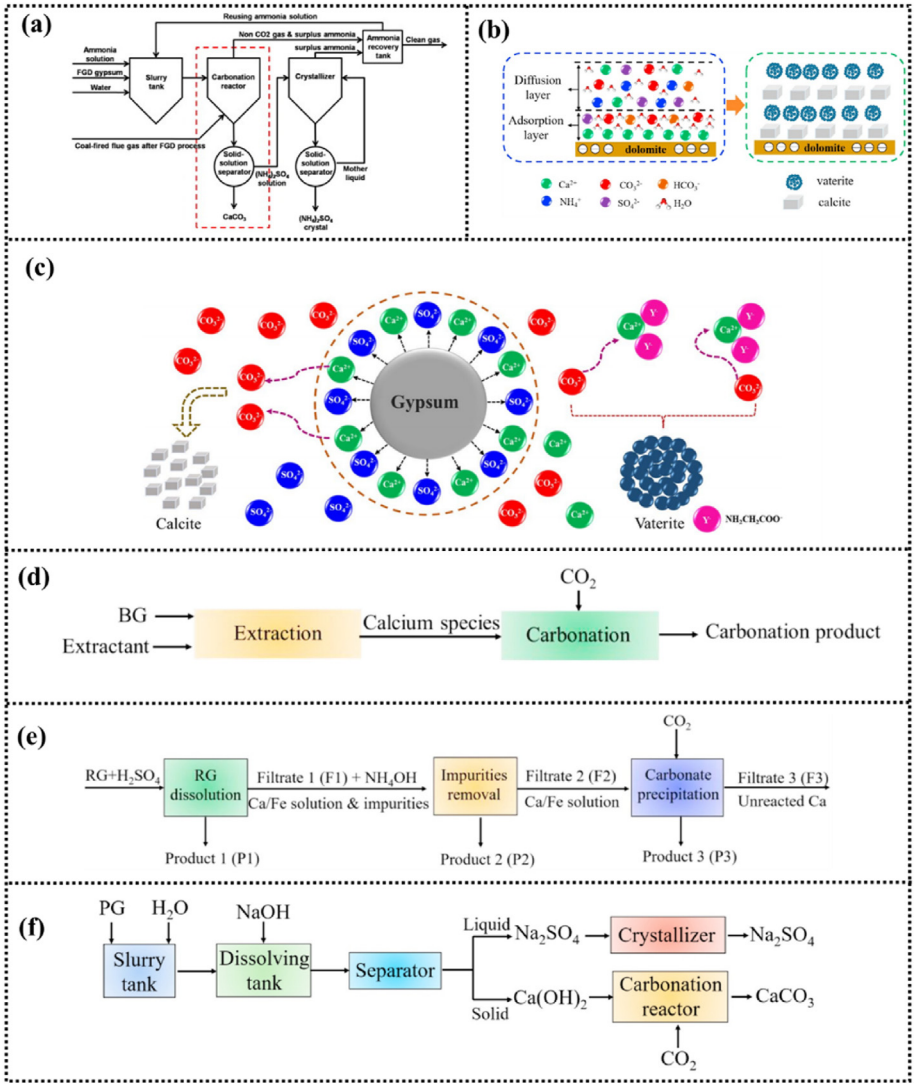

Fig. 5. (a) Direct aqueous carbonation of FGDG [85]. (b) The generation mechanism for polymorph $CaCO_3$ from $CaSO_4 \cdot 2H_2O$ carbonation in the presence of dolomite [18]. (c) The formation mechanism of vaterite by carbonation of waste gypsum in the presence of glycine [86]. (d) The process of the indirect aqueous mineral carbonation of byproduct gypsum (RG) [39]. (e) Schematic diagram of the indirect aqueous mineral carbonation of RG via the pH-swing process [87]. (f) Flowchart of the indirect aqueous mineral carbonation of PG using NaOH as the leaching agent [2].

carbonation efficiency and polymorph of $CaCO_3$, including the type of raw material, temperature, alkaline medium, impurities, CO_2 flow rate, and auxiliary processes [88]. Lee et al. [85] conducted a systematic study on the effects of ammonia concentration, CO_2 flow rate, solid−liquid ratio, and CO_2/N_2 concentration on the conversion rate of FGDG. The results showed that as the ammonia concentration increased, the conversion rate of FGDG also increased gradually, eventually surpassing 95% within 10 min. Zhao et al. [89] proposed a new technique to enhance the carbonation efficiency of PG under high-concentration CO_2 conditions using a pressurized method. The findings revealed that under a CO_2 partial pressure of 0.8 MPa, a liquid−solid ratio of 1:1, a stirring speed of 300–500 r min^{-1}, and an initial temperature of 80 °C, the carbonation efficiency of PG reached approximately 97.5% within 5−10 min. The presence of Fe_2O_3 in TG results in a carbonation product that is a combination of $CaCO_3$ and $FeCO_3$. A study revealed that at atmospheric pressure, the carbonation efficiency of TG is less than 5%. However, when the partial pressure of CO_2 is increased to 70 bar, the conversion rates of Fe and Ca increase to 26.31% and 41.04%, respectively [90]. Comparatively, FGDG and PG exhibit a higher carbonation efficiency and lower impurity content in the $CaCO_3$ products. Lee et al. [91] conducted an experiment in which they mineralized FGDG in an ammonia medium, resulting in a mixture of calcite and vaterite. The reaction temperature significantly influenced the polymorph of $CaCO_3$. Calcite and vaterite are the carbonation products when the reaction temperature is 20 °C and 40 °C, respectively. With an increase in temperature to 60 °C, aragonite starts to appear in the product, and the content of calcite becomes higher than that of vaterite. At 80 °C, the product consists solely of calcite and aragonite. Additionally, when NaOH is used as the alkaline medium, the main product obtained from the mineral

Table 4
Preparation of $CaCO_3$ by CO_2 mineralization of waste gypsum under different processes.

Carbonation pathway	Gypsum type	Leaching agent	Polymorph modifier	Temperature (°C)	Pressure (bar)	Time (min)	Liquid-solid ratio (mL g^{-1})	Ca^{2+} leaching rate(%)	Polymorphs	$CaCO_3$ Yield (g kg^{-1})	References
Direct carbonation	PG	$NH_3 \cdot H_2O$	/	30−40	1.0	60	8	/	C	/	[10]
	FGDG	$NH_3 \cdot H_2O$	/	Room temperature	1.0	50	6.67	/	C/V	/	[77]
	FGDG	$NH_3 \cdot H_2O$ TEA HMT	/	80	1.0	20	/	/	C	/	[84]
	FGDG	$NH_3 \cdot H_2O$	/	Room temperature	1.0	10	1	/	C/V	/	[85]
	FGDG	$NH_3 \cdot H_2O$, Glycine	Glycine	25	1.0	30	2.5−20	/	V	/	[86]
	PG	$NH_3 \cdot H_2O$	/	80	8.0	5	2	/	C	/	[89]
	RG	$NH_3 \cdot H_2O$	/	200	20	60	5	/	C/V	/	[90]
	FGDG	$NH_3 \cdot H_2O$	/	20−80	1.0	60	/	/	C/A/V	/	[91]
	FGDG	$NH_3 \cdot H_2O$	/	Room temperature	1.0	60	/	/	C	/	[92]
	FGDG	$NH_3 \cdot H_2O$	/	Room temperature	1.0	15	3−200	/	C	/	[93]
	FGDG	$NH_3 \cdot H_2O$	/	Room temperature	1.0	60	10	/	C/V		[96]
	FGDG	NaOH	/	20	1.0	120	13	/	C	/	[99]
	FGDG	$NH_3 \cdot H_2O$	Polyacrylic acid	Room temperature	1.0	90	6.5	/	C	/	[100]
	FGDG	$NH_3 \cdot H_2O$	/	25	1.0	30	10	/	V	227.3	[101]
Indirect carbonation	PG	CH_3COONH_4	$NH_3 \cdot H_2O$	20−50	1.0	60	10	98.1	V	510.0	[95]
	PG	CH_3COONH_4	$NH_3 \cdot H_2O$	60	1.0	60	10	98.1	V/A	510.0	[95]
	PG	KOH	/	Room temperature	1.0	15	20	/	V/C	731.8	[102]
	PG	NaOH	/	Room temperature	1.0	60	20	96.0	V/C	/	[103]
	PG	NaOH		Room temperature	1.0	15	4	97.4	V/C	500.0	[104]

carbonation of FGDG is calcite [84]. The difference in the polymorph of $CaCO_3$ between the two alkaline media is primarily attributable to the presence of NH_4^+ [92]. Wang et al. [18] investigated the influence of impurities, such as dolomite, on the polymorph of $CaCO_3$ during the mineral carbonation of FGDG (Fig. 5b). They observed that the content of calcite in the product initially increases and then decreases with increasing dolomite content. When the dolomite content reaches 1.0 wt%, the proportion of calcite reaches its peak value (approximately 27%). Correspondingly, the vaterite content first decreased and then increased. They believe that a high-density water layer forms on the surfaces of dolomite due to its hydrophilicity, leading to more ions being dissolved. Moreover, negatively charged dolomite preferentially adsorbs Ca^{2+} through electrostatic attraction, resulting in a locally high proportion of Ca^{2+}/CO_3^{2-}. Additionally, according to the diffusion bilayer theory, adsorption and diffusion layers form on the surface of dolomite particles. Therefore, the adsorption layer on the surface of the dolomite particles creates a greater local proportion of Ca^{2+}/CO_3^{2-} than does the diffusion layer. A higher Ca^{2+}/CO_3^{2-} ratio is beneficial for the formation of calcite. When the concentration of dolomite particles reaches a certain threshold, excessive amounts of dolomite particles may adsorb dissolved Ca^{2+}. Since the dissolved Ca^{2+} remains constant, this leads to a decrease in the local Ca^{2+}/CO_3^{2-} ratio, weakening the induction effect and thus reducing the content of calcite. The hydrophilicity and surface negative charge of impurity dolomite particles play a crucial role in the formation of calcite. Song et al. [77,93,94] systematically studied the effects of the CO_2 flow rate, $NH_3\cdot H_2O$ concentration, and solid−liquid ratio on the polymorph of $CaCO_3$ during mineral carbonation of FGDG. The results indicate that when $NH_3\cdot H_2O$ is in excess, the carbonation product is vaterite, whereas calcite is the product when $NH_3\cdot H_2O$ is present in an appropriate amount according to stoichiometry. Ding et al. [95] studied the influence of operating parameters on the polymorph of $CaCO_3$ in a three-phase reaction system involving $CaSO_4\cdot 2H_2O$, $NH_3\cdot H_2O$, and CO_2. They discovered that when the temperature exceeded 30 °C, the CO_2 flow rate was less than 150 mL min^{-1}, the $NH_3\cdot H_2O$ concentration was less than 2%, and the main product was calcite. In contrast, a product composed mainly of spherical microporous vaterite with a purity of 99% was obtained at a reaction temperature of 25 °C, $NH_3\cdot H_2O$ concentration of 8%, and CO_2 flow rate of 250 mL min^{-1}. Cheng et al. [96] investigated the influence of ultrasound on the polymorph of $CaCO_3$ in the same reaction system. The findings revealed that while the carbonation product is a mixture of calcite and vaterite, ultrasound significantly reduces the particle size of $CaCO_3$ and increases the vaterite content in the product from 60% to 80%. Polymorph modifiers also influence the polymorph of $CaCO_3$. Luo et al. [97] examined the effect of aspartic acid on the nucleation and growth of $CaCO_3$ in a $Ca(OH)_2$–CO_2 reaction system. They determined that the complexation reaction between aspartic acid and $Ca(OH)_2$ results in the formation of vaterite. Furthermore, aspartic acid adsorbs on the surface of vaterite, preventing its transformation into calcite through a dissolution recrystallization process. Using the same reaction system, Lai et al. [98] investigated the effects of alanine, leucine, aspartic acid, and glycine on a polymorph of $CaCO_3$. They proposed that glycine induces the formation of monodisperse vaterite, with complexation between glycine and Ca^{2+} playing a key role in the formation of vaterite. Similarly, Liu et al. [86] reached a similar conclusion and reported that glycine significantly increased the vaterite content in products obtained from the mineral carbonation of FGDG. The vaterite content gradually increases with the concentration of glycine until it reaches a maximum value of approximately 97% at a glycine concentration of 20%. Based on these findings, the research team proposed the process mechanism of glycine-mediated mineral carbonation for the selective preparation of vaterite from FGDG (Fig. 5c). They postulated that the carbonation reaction generates complex calcium $Ca(NH_2CH_2COO)_2$, which then ionizes into free Ca^{2+}. As CO_2 continues to diffuse into the system, CO_3^{2-} accumulates, and $CaCO_3$ precipitates when the $CaCO_3$ solution becomes saturated. In the initial stages, the concentration of CO_3^{2-} in the reaction system is relatively low, facilitating the formation of calcite with free Ca^{2+}. As the concentration of CO_3^{2-} increases, it tends to react with Ca^{2+} in $Ca(NH_2CH_2COO)_2$, resulting in the formation of vaterite.

The indirect carbonation process for waste gypsum involves two steps. First, acid, alkali, and other extractants are used to extract the active component Ca^{2+}/Mg^{2+} from desulfurization gypsum. Then, Ca^{2+}/Mg^{2+} reacts with CO_2 to generate carbonate (Fig. 5d). Compared to the direct carbonation process, the indirect carbonation process can remove impurities before the carbonation reaction, resulting in higher purity $CaCO_3$. In the indirect carbonation route (Table 4), leaching agents are the main factors affecting the carbonation efficiency, product purity, and operating costs. The indirect carbonation process of waste gypsum using H_2SO_4 and NaOH as leaching agents is shown in Fig. 5e and f. However, when NaOH or H_2SO_4 is used as a leaching agent to extract Ca^{2+} from waste gypsum, impurities such as SiO_2, Fe_2O_3, and Al_2O_3 are transferred directly to the leaching solution, leading to a decrease in the purity of $CaCO_3$. To address this issue, Ding et al. [95] employed ammonium acetate to separate Ca^{2+} and concentrate impurity ions from PG. They also investigated the influence of operating parameters on salt leaching and carbonation results. The results showed that the calcium leaching rate and carbonation efficiency reached 98.1% and 98.32%, respectively. Various polymorphs and morphologies of $CaCO_3$ were synthesized by adjusting the carbonation temperature and ammonia concentration, and the spherical vaterite met the recommended Chinese standard (HG/T 2226–2010).

In comparison to indirect carbonation methods, direct carbonation of waste gypsum has gained significant attention due to its simple operation. However, there is still much work to be done, such as enhancing the carbonation process and increasing the capacity for CO_2 sequestration in the direct carbonation process of waste gypsum. To gain a deeper understanding of the effect of impurities on the nucleation and

growth of $CaCO_3$ at the molecular level, it is necessary to conduct molecular dynamics simulations of the carbonation reaction process. In addition, although modifiers play a crucial role in regulating the polymorph and morphology of $CaCO_3$, their addition results in increased operating costs. Therefore, further research is needed to explore inexpensive modifiers.

2.4. Fly ash

Fly ash (CFA) is a byproduct of coal combustion for power generation. In China, the annual production of CFA is approximately 620 million tons, which accounts for more than 50% of the global production. Improper disposal of CFA can result in significant environmental pollution and ecological damage due to its high alkalinity. Currently, CFA is primarily utilized in the building materials industry, including cement, concrete, and road paving. However, this technology faces the challenge of low product value. The comprehensive utilization rate of CFA in China has remained at approximately 65% in recent years. Therefore, it is crucial to explore new approaches for the resource utilization of CFA. Both CFA and CO_2 are generated at coal-fired power plants. Consequently, utilizing CFA for CO_2 sequestration can not only reduce transportation costs but also substantially decrease CO_2 emissions from power plants. Table 5 presents the research progress on the synthesis of $CaCO_3$ from CFA under various process conditions.

Fig. 6a illustrates the direct aqueous carbonation of CFA. This technology is relatively simple and cost-effective. However, the Ca in CFA primarily exists in the form of Ca–Si–Al–O, Ca–Si–O, and $CaCO_3$, resulting in its low reactivity. Despite its thermodynamic advantage, mineral carbonation by CFA suffers from limited reaction kinetics. To address the slow dissolution of CO_2 and extraction of Ca^{2+}/Mg^{2+} in mineral carbonation, various reaction pathways have been developed.

In the integrated CO_2 absorption and mineralization process (Fig. 6b), amines react with CO_2 to generate a CO_2-rich solution. The reaction kinetics of this process are significantly greater than those of the CO_2 hydration pathway due to the strong affinity of amines for CO_2 [105,106]. Industrial wastes are then added to the solution to induce CO_2 desorption from the amines and promote the synthesis of $CaCO_3$ [48]. An amine-looping process has also been developed to integrate CO_2 absorption and mineralization into a single step [107,108]. In this process, industrial wastes, CO_2, and alkaline reagents such as amines and amino acid salts are added to a single reactor [108]. During this process, alkaline reagents quickly transport CO_2 from the gas phase to the liquid phase and react with Ca^{2+} to generate $CaCO_3$, effectively regenerating it in-situ [109]. However, in the aforementioned two processes, separating the newly synthesized $CaCO_3$ products from the waste residue after calcium extraction is challenging, leading to a decrease in the purity of $CaCO_3$ [110]. The slow reaction kinetics and low purity of $CaCO_3$ are key factors limiting the development of the direct carbonation route.

Table 5
Preparation of $CaCO_3$ by CO_2 mineralization of CFA under different processes.

Carbonation pathway	Leaching agent	Polymorph modifier	Temperature (°C)	Pressure (bar)	Time (min)	Liquid-solid ratio (mL g^{-1})	Ca^{2+} leaching rate (%)	Polymorphs	$CaCO_3$ Yield (g kg^{-1})	References
Direct carbonation	H_2O	/	Room temperature	1.0	30	20–100	/	C	36.36	[110]
	H_2O	/	40	20	/	5	/	C	234.1	[127]
	H_2O	/	20–60	10–40	120	6.67–20	/	C	59.1	[128]
Indirect carbonation	Glycine	Glycine	Room temperature	1.0	15–60	5	51.1	V	114.8	[48]
	L-alanine	L-alanine	Room temperature	1.0	15–60	5	34.2	V	78.2	[48]
	L-arginine	L-arginine	Room temperature	1.0	15–60	5	21	C	54.5	[48]
	Glycine	Glycine	25	1.0	60	10	42.17	V	89.1	[72]
	Piperazine	Piperazine	55	1.0	90	10	/	C/A	233.9	[109]
	NH_4Cl	/	60	1.0	40	6	36	/	471.7	[112]
	HNO_3	/	Room temperature	1.0	150	20	25.8–72.6	C	25.0	[113]
	NH_4Cl, NH_4NO_3, CH_3COONH_4	/	25–90	1.0	120	20	35–41	C/V	170.0	[114]
	Glycine	Glycine	25	1.0	60	5	38.7	V	98.8	[116]
	Protonated amine	EA, MDEA, TEA, AMP, DMEA, DEEA, MPA, and 1,3-DAP	25	1.0	60	6.25	8–12	V	30–50	[123]
	Protonated amine	DEA, PZ, TMEDA	25	1.0	60	6.25	8–12	C	30–50	[123]
	HCl	Diisobutylamine, 1-octanol	25	1.0	60	3.0	/	C/V	282.4	[125]
	CH_3COOH	/	60	10.0	60	10	/	C	600.0	[129]
	NaCl	/	30	1.0	60	20	9.65	/	59.77	[130]

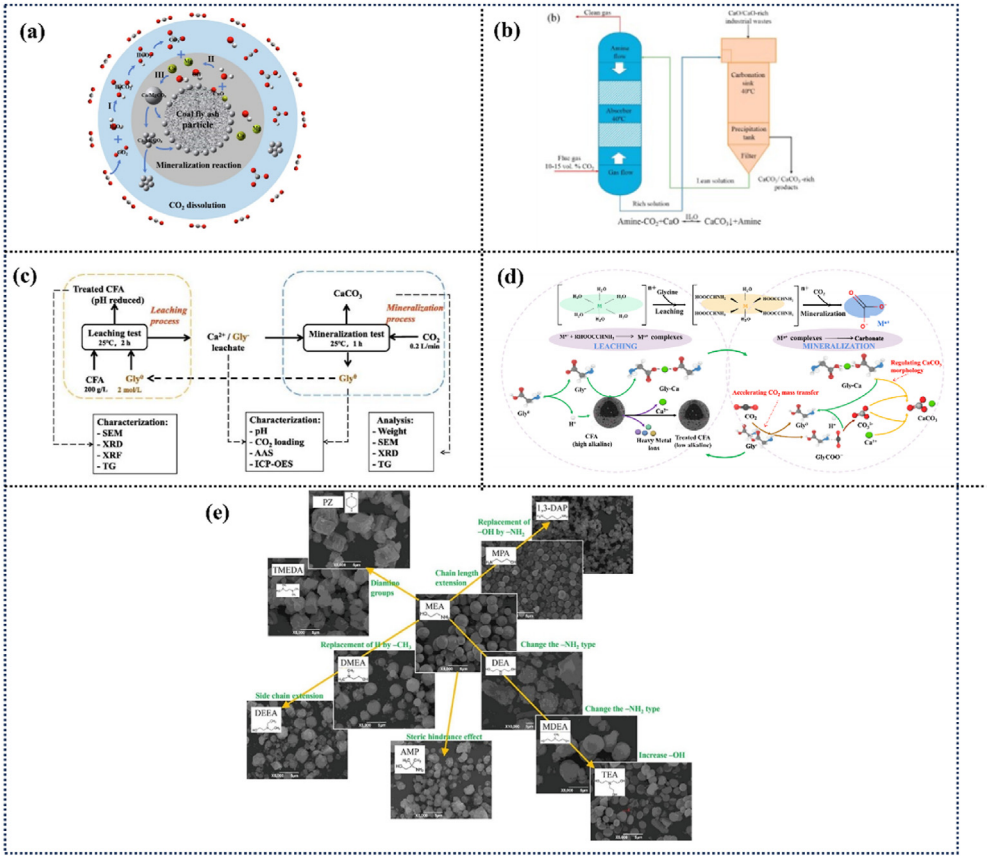

Fig. 6. (a) Direct aqueous carbonation mechanism of CFA [126]. (b) Integrated processes of CO_2 uptake and mineralization [10]. (c) An amino acid-mediated leaching-mineralization cycle (LMC) route [116]. (d) Mechanism of the leaching-mineralization cycle (LMC) process of glycine in CFA [72]. (e) Effect of amines on the morphology of $CaCO_3$ [123].

Additionally, calcite or aragonite is typically produced during the direct carbonation process of CFA [109,110].

To address this challenge, a pH-swing process was developed. In the indirect carbonation process, Ca^{2+}/Mg^{2+} is initially leached from CFA using recyclable acids such as NH_4Cl, NH_4NO_3, CH_3COONH_4, NH_4HSO_4 $(NH_4)_2SO_4$, sodium acetate, sodium citrate, and sodium oxalate, followed by a liquid−solid separation [111–113]. These agents not only provide protons for mineral dissolution but also chelate ions to improve the availability of Ca^{2+}/Mg^{2+} for subsequent carbonation reactions. He et al. [114] extracted Ca^{2+} from CFA using ammonium acetate (CH_3COONH_4), ammonium chloride (NH_4Cl), and ammonium nitrate (NH_4NO_3), and reported that the leaching rate of calcium ions reached 35%–40% within 1 h at 25 °C. Increasing the leaching temperature and concentration of leaching agents can enhance Ca^{2+} leaching. Hosseini et al. [112] investigated the indirect carbonation process of brown coal fly ash using NH_4Cl as a leaching agent. The leaching rate of Ca^{2+} in brown coal fly ash is approximately 35% within 1 h at 80 °C. In the carbonation stage, CO_2 is introduced into the leachate, and the carbonation efficiency of Ca^{2+} is only approximately 40%. Despite effective leaching, the acidity of the leachate is unsuitable for subsequent CO_2 absorption and carbonation reactions. It is well known that low pH values are advantageous for leaching alkaline earth metals from alkaline solid wastes, while high pH values are conducive to CO_2 mineralization and carbonate precipitation. To facilitate CO_2 absorption and $CaCO_3$ precipitation, alkaline reagents such as NaOH and NH_4OH need to be added to the leachate [87,115]. Moreover, the addition of these alkaline reagents also helps remove some impurity elements from the leachate, thereby improving the purity of ultrafine $CaCO_3$. However, Zheng's group [48,72,116] believes that the extensive consumption of reagents, the complex process and high energy consumption of acid and alkali recovery, and frequent pH-swing operations restrict the practical application of this method. They proposed an amino acid-mediated leaching-mineralization cycle (LMC) strategy (Fig. 6c) that facilitates Ca^{2+} leaching, promotes CO_2 absorption, increases $CaCO_3$ production, and controls $CaCO_3$ morphology. The results indicate that the leaching efficiency ranges from 38.7% to 51.1% and the vaterite yield for fly ash ranges from 89.10 to 114.8 g kg^{-1} under mild conditions. The mechanism of the LMC process using glycine and CFA is depicted in Fig. 6d. Glycine(Gly^0), as a pH buffer, provides a suitable pH for the leaching of Ca^{2+} from alkaline solid wastes and the production of Gly^- during the leaching step. Additionally, Gly^0, as a leaching ligand, can enhance the dissolution of Ca^{2+} in solution by forming a $Ca^{2+}-Gly^0$ complex. During the mineralization process, Gly^- acts as an effective CO_2 absorbent,

accelerating the mass transfer of CO_2 from the gas phase to the liquid phase and maintaining high concentrations of CO_2-bearing species such as CO_3^{2-}, HCO_3^-, and carbamate in the leachate. Ca^{2+} reacts with CO_3^{2-} to produce high-purity $CaCO_3$, while Gly^- is simultaneously regenerated to Gly^0. Furthermore, the presence of Gly^- species, which serve as polymorph modifiers of $CaCO_3$, hampers the dissolution of unstable vaterite into stable calcite. Previous studies have shown that the polymorph and morphology of $CaCO_3$ during the carbonation process can be controlled by adjusting the CO_2 supersaturation and pH and adding modifiers to the solution [105,117–121]. Notably, organic modifiers with functional groups such as −OH, $-NH_2$, and −COOH significantly influence the polymorph and morphology of $CaCO_3$ by complexing with Ca^{2+} and adsorbing to particular surfaces of $CaCO_3$ crystals [122]. For instance, Huang et al. [123] selected protonated amines with various amino types and side-chain lengths as modifiers and systematically studied the influence of amino groups on Ca^{2+} leaching from CFA, carbonation performance, and nucleation/growth of $CaCO_3$. They found that these alkaline amines accelerated Ca^{2+} leaching and exhibited excellent performance in controlling the size, polymorph, and morphology of the $CaCO_3$ product. The influence of amines on the $CaCO_3$ polymorph is shown in Fig. 6e. DEA, PZ, and TMEDA induced the formation of calcite, while EA, MDEA, TEA, AMP, DMEA, DEEA, MPA, and 1,3-DAP favored the production of vaterite. In other words, the primary amino group had a more pronounced effect on vaterite stabilization than did the secondary and tertiary amino groups. Introducing a side chain could expedite the conversion of vaterite to calcite, and increasing the chain length could decrease the particle size of vaterite. In another study, Madhav et al. [124] successfully synthesized calcite particles by adding polyvinyl pyrrolidone and sodium dodecyl sulfate with active functional groups to a carbonation reaction system. Furthermore, Chen et al. [125] proposed a leaching-mineralization-regeneration process for CO_2 sequestration and $CaCO_3$ production from CFA mediated by diisobutylamine. When the diisobutylamine/1-octanol/leaching solution ratio was set at 1:2:3, the authors achieved nearly complete precipitation of Ca and a high vaterite yield of 282.4 g kg^{-1}. The purity of vaterite (99.1%) met the recommended Chinese standard (HG/T 2226–2019).

In conclusion, the preparation of ultrafine $CaCO_3$ using the abovementioned four common industrial solid wastes is technically feasible. This process not only facilitates the resource utilization of solid wastes but also helps in reducing CO_2 emissions to some extent. Efficient and rapid extraction of Ca^{2+} from solid wastes is a crucial aspect of this technology. Currently, recyclable reagents are often employed as leaching agents instead of strong acids. However, the leaching rate is limited under the same conditions, resulting in slow reaction kinetics and the inability to achieve high leaching rates within a short period. The leaching kinetics of Ca^{2+} are primarily influenced by temperature, the concentration of the leaching agent, and the solid−liquid ratio. Kinetic models can be utilized to predict the actual extraction process and adjust the operating parameters to achieve rapid and effective extraction of Ca^{2+} [131]. Another important aspect of this technology is the selection of appropriate polymorph modifiers to regulate the nucleation and growth of $CaCO_3$ during the carbonation stage. According to classical nucleation theory, the addition of modifiers can disrupt the interactions between ions in the lattice, thereby affecting the thermodynamic stability of the newly formed phase [132]. Combined with the control of carbonation reaction parameters, it is possible to produce vaterite with relatively small particle sizes.

3. Potential industrial applications of the preparation of $CaCO_3$ from industrial wastes

The preparation of ultrafine $CaCO_3$ through CO_2 mineralization using industrial solid wastes is a promising technology for reducing CO_2 emissions. Significant research has been conducted on this technology at the laboratory scale in recent years. However, only a few methods have progressed to pilot and commercial-scale applications. In 2014, Finland designed, constructed, and tested the world's first mineral carbonation pilot plant. This plant converts steel slag and CO_2 into precipitated $CaCO_3$ (PCC) and was tested in Finland in 2014 [133]. The plant operates in batch mode and can handle up to 20 kg of steel slag and 190 L of NH_4Cl solvent, producing approximately 10 kg of $CaCO_3$ per batch. In the leaching stage, a 1 mol L^{-1} NH_4Cl solution is used to leach the active calcium component in the steel slag, achieving an 80% leaching efficiency. In the subsequent carbonation stage, the maximum carbonation efficiency reached 71% under optimal conditions. The resulting $CaCO_3$ consists mainly of calcite and aragonite, with a purity as high as 99.5%. The NH_4Cl solution is recycled and reused for leaching calcium from steel slag after carbonation, enhancing the economic feasibility of the process. However, the calcium extraction efficiency decreased to 39% after more than ten cycles of reusing the NH_4Cl solvent.

Iizuka et al. [134] conducted a pilot-scale plant operation for the treatment of concrete sludge and the production of $CaCO_3$. The process involved introducing the concrete sludge into a calcium extraction reactor and diluting it with water. The resulting slurry was then agitated to facilitate the simultaneous hydration of unhydrated cement and extraction of calcium. After a specified duration of stirring, the solids were separated from the liquid using a filter press, and the filtrate was transferred to a $CaCO_3$ crystallization reactor. Flue gas enriched with CO_2 was introduced to the reactor, where it reacted with the Ca-rich solution to produce high-purity $CaCO_3$ (> 97%) suitable for a range of industrial and commercial applications. Over the course of one week, the plant processed 356.7 tons of concrete sludge and sequestered 0.140 tons of CO_2 from boiler emissions. An analysis of the power consumption and CO_2 sequestration of the pilot-scale plant showed a reduction in net CO_2 emissions of 118 kg. The mineral carbonation process employed in this plant proves advantageous for mitigating global warming, as it operates at standard temperatures and pressures and eliminates the need

for CO_2 purification or pressurization. In another study, Park et al. [135] developed a pilot-scale reactor with a total $CaCO_3$ production capacity of 20 kg d^{-1}. The process involved utilizing 0.5 mol L^{-1} HCl for the extraction of calcium from waste concrete. The pH of the solution was then adjusted to 11.5 using NaOH to remove impurities. Subsequently, CO_2 was injected into a 100 L reactor at a rate of 10 L min^{-1}. This setup achieved a production efficiency of 96% $CaCO_3$ within a CO_2 injection duration of 30 min, and the calcium concentration in the synthesized $CaCO_3$ reached 99.0%.

Xie et al. [136] demonstrated the conversion of PG to $CaCO_3$ and $(NH_4)_2SO_4$ through CO_2 mineralization by employing a pilot-scale device with a capacity of 100 Nm^3 h^{-1}. The process involved cooling the flue gas to 50 °C using circulating water and treating it with ammonia to reduce the CO_2 concentration from 15% to 4.5%. The ammonia-treated liquid was then subjected to mineralization with PG, resulting in a 90% conversion rate at 75 °C over a period of 6 h. This process produced $CaCO_3$. The remaining solution was evaporated to achieve a 45% concentration of $(NH_4)_2SO_4$, which was subsequently crystallized to obtain granular $(NH_4)_2SO_4$ fertilizer. The estimated revenue from this conversion process per ton of CO_2 is approximately $17 USD.

The Process Institute of the Chinese Academy of Sciences [137] has conducted extensive research on the indirect mineralization of steel slag for the production of microfine $CaCO_3$. This research has resulted in notable technological advancements and engineering demonstrations. A multiphase composite media pretreatment of steel slag has been developed using acetic acid and other weak acid media to facilitate the leaching of effective calcium components. The leached calcium components are then subjected to pressurized carbonation, converting them into high-quality $CaCO_3$ products. Furthermore, the process includes the simultaneous recovery of multiphase composite reaction media, the optimization of resource utilization and the enhancement of sustainability. Presently, a 5000 t a^{-1} pilot production line for the preparation of aragonite from steel slag has been established in Huai'an city, Jiangsu Province, China [138].

In recent decades, various carbonation routes have been developed to facilitate the large-scale application of mineral carbonation. Despite these advancements, the industrial utilization of waste for producing $CaCO_3$ faces significant challenges, including high energy consumption, low carbonation efficiency, substantial costs, difficulties in controlling the crystal form, and low purity of the final product. To overcome these obstacles, ongoing optimization of process conditions and the development of straightforward, cost-effective technologies are critical.

4. Economic analysis of mineral carbonation process

The economic analysis of mineral carbonation process is crucial for develop forward of this technology. Generally speaking, the energy consumption and operating costs in mineral carbonation are closely related to plant size, pretreatment like the grinding and thermal treatment of raw materials, operation conditions, leaching agents and separation/disposal of the carbonation products [139].

When using natural minerals such as olivine, wollastonite and serpentine as raw materials, the cost of the direct aqueous carbonation process with pretreatments was estimated to be in the range of $50–210 per t CO_2 [140]. The total cost of the mineral carbonation process developed by National Energy Technology Laboratory was approximately $54 per t CO_2 avoided, and this technology reduced the energy requirement for thermal-activation by 63% by using thermal energy instead of electrical energy and coupling to partial dihydroxylation with heat integration [141,142]. Li and Hitch [143] conducted an economic analysis on the integration of mineral carbonation and mining operations, and the cost of the direct aqueous carbonation by using mineral wastes was in the range of $104–107 per t CO_2. In this method, the carbonation efficiency reached 60%, and about 14.6 Mt CO_2/year can be sequestered by using these wastes.

Moreover, when using industrial wastes like concrete wastes and steel slag as raw materials, the cost of the direct aqueous carbonation was in the range of $8–104 per t CO_2 which is closely related to the operating parameters [144,145]. For example, the estimated cost of mineral carbonation for steel slag is around $125 per t CO_2 net avoided [145].

The cost of indirect mineral carbonation process is usually higher than the direct route because additional leaching agents such as inorganic acids, organic acids, bases, and ammonium salts are required to extract Ca species from natural minerals or industrial wastes [146]. In this process, the estimated cost of leaching agents was in the range of $600–1600 per t CO_2 without regenerating the leaching agents [147]. Futhermore, CO_2 emissions in the regeneration process of leaching agents was about 3 times higher than the CO_2 sequestration capacity during the carbonation process [148].

For direct aqueous carbonation route, the cost can be calculated by subtracting the cost of input materials from the cost of output materials [82]. Taking the direct carbonation process of FGDG as an example, in FGDG-NaOH-CO_2 system, the cost of input materials (including FGDG, NaOH, and CO_2) was 125.4 $ t^{-1}, while that of output materials (including $CaCO_3$ and Na_2SO_4) was 430.5 $ t^{-1} [82]. Thus, the profit was 305.1 $ t^{-1}. In FGDG-$NH_3 \cdot H_2O$–CO_2 system, the cost of input materials (including FGDG, $NH_3 \cdot H_2O$, and CO_2) was 415.6 $ t^{-1}, while that of output materials (including $CaCO_3$ and $(NH_4)_2SO_4$) was 842.5 $ t^{-1} [82]. Thus, the profit was 426.9 $ t^{-1}. The calculation results indicate that direct aqueous carbonation of FGDG was a cost-effective and an environmentally friendly method or sequestering CO_2. In addition, the profit can also be calculated based on the difference between the cost of input and output materials to sequester 1 ton of CO_2.

For the indirect carbonation process of TG, additional leaching agents and operations were employed to extract the reactive species from waste gypsum. The cost can be calculated by subtracting all cost of output including the items and energy from all cost of input including the items and energy [149]. In this process, the costs of $NH_3 \cdot H_2O$ and H_2SO_4 were

$97.0 and $89.8, respectively, which accounts for 89.6% of the total cost. In addition, the cost of deionized water was $21.66. The energy cost of other processes such as filtration and crushing was $5.98. The cost of transportation was $11. The total value of the products obtained from this process is $158.6. Thus, the cost for mineral carbonation of TG was $66.82 per t CO_2 avoided.

5. Conclusions

Mineral carbonation of industrial solid wastes can simultaneously address solid waste management and CO_2 emission reduction while producing high-value ultrafine $CaCO_3$ products. Crystalline $CaCO_3$ includes three polymorphs: vaterite, aragonite, and calcite, in order of increasing thermodynamic stability. $CaCO_3$ with different crystal forms has different application scenarios. Thus, the controllable preparation of $CaCO_3$ through mineral carbonation of industrial wastes has been widely studied.

The polymorph of $CaCO_3$ synthesized by carbonation process is determined the combined effects of various factors such as liquid-to-solid ratio, solution pH, CO_2 flow rate, reaction temperature, residence time, and polymorph modifiers. These parameters essentially impact the nucleation and growth of $CaCO_3$ by altering the CO_2 supersaturation in the reaction system and the surface energy of $CaCO_3$ grains. Increasing the initial pH of the solution and the CO_2 flow rate favors the formation of vaterite, but calcite is formed under excessively high pH. Vaterite formation is favored at lower temperatures and residence time. As the temperature increases and the residence time prolongs, it passes through aragonite metastable phase and eventually transforms into calcite. In general, the addition of polymorph modifiers during carbonation can decrease the surface energy of $CaCO_3$ grains, facilitating the synthesis of vaterite.

The past decade has witnessed tremendous advances in experimental strategies for the controllable preparation of $CaCO_3$ by industrial solid wastes, but several challenges still require further research.

(1) Research on producing $CaCO_3$ from industrial waste has shown promising results at the laboratory scale, but its industrial application remains unconfirmed. The primary challenges for scaling up this technology include high costs, high energy consumption, low carbonation efficiency, and low product yield. Consequently, further studies are needed to enhance the carbonation process and understand the reaction kinetics and the kinetics of $CaCO_3$ nucleation and crystallization.
(2) Direct aqueous carbonation and indirect carbonation are the two most extensively studied carbonation routes. While indirect carbonation can produce high-purity $CaCO_3$, the development of cost-effective leaching agents, increasing the calcium leaching rate, and achieving solvent regeneration are critical issues that need further exploration.
(3) Vaterite is thermodynamically unstable and readily transforms into aragonite and calcite in humid environments or aqueous solutions. To achieve controlled synthesis of $CaCO_3$, continuous adjustment of the experimental parameters and the use of polymorph modifiers are typically necessary. These measures help regulate the crystallization process and obtain $CaCO_3$ products with specific polymorphs and morphologies. Therefore, a thorough understanding of $CaCO_3$ nucleation and growth, as well as the logic behind various influencing factors, is crucial for customizable synthesis.
(4) Limited studies have utilized life cycle assessment (LCA) techniques to evaluate the environmental impacts and energy consumption associated with $CaCO_3$ preparation from industrial solid waste. Employing LCA to assess comprehensive environmental impacts and resource consumption can reveal detailed trends in resource utilization and emissions, facilitating comparisons between different products or processes and aiding decision-making within the industry.

Ethical approval

This article does not contain any studies with human participants or animals performed by any of the authors.

CRediT authorship contribution statement

Run Xu: Supervision. **Fuxia Zhu:** Writing − original draft. **Liang Zou:** Conceptualization. **Shuqing Wang:** Data curation. **Yanfang Liu:** Writing − review & editing. **Jili Hou:** Supervision. **Chenghao Li:** Investigation. **Kuntong Song:** Validation. **Lingzhao Kong:** Writing − review & editing. **Longpeng Cui:** Project administration. **Zhiqiang Wang:** Writing − review & editing.

Declaration of competing interest

The authors declare that they have no known competing financial interests or personal relationships that could have appeared to influence the work reported in this paper.

Acknowledgements

Financial support was received the Science & Technology Foundation of RIPP (PR20230092, PR20230259), the National Natural Science Foundation of China (22278419), and the Key Core Technology Research (Social Development) Foundation of Suzhou (2023ss06).

References

[1] Z. Zhang, S.Y. Pan, H. Li, J.C. Cai, A.G. Olabi, E.J. Anthony, V. Manovic, Renew. Sustain. Energy Rev. 125 (2020) 109799.
[2] C. Cardenas-Escudero, V. Morales-Florez, R. Perez-Lopez, A. Santos, L. Esquivias, J. Hazard. Mater. 196 (2011) 431–435.
[3] H. Xie, L. Tang, Y. Wang, T. Liu, Z. Hou, J. Wang, T. Wang, W. Jiang, P. Were, Environ. Earth Sci. 75 (2016) 615.
[4] W.T. Liu, L.M. Teng, S. Rohani, Z.F. Qin, B. Zhao, C.C. Xu, S. Ren, Q.C. Liu, B. Liang, Chem. Eng. J. 416 (2021) 129093.

[5] Y.-Q. Niu, J.-H. Liu, C. Aymonier, S. Fermani, D. Kralj, G. Falini, C.-H. Zhou, Chem. Soc. Rev. 51 (2022) 7883–7943.
[6] Q. Huang, Y. Liu, Z. Ouyang, Q. Feng, Bioact. Mater. 5 (2020) 980–989.
[7] C.S. Poon, P. Shen, Y. Jiang, Z. Ma, D. Xuan, Cement Concr. Res. 173 (2023) 107284.
[8] D.B. Trushina, T.N. Borodina, S. Belyakov, M.N. Antipina, Mater. Today Adv. 14 (2022) 100214.
[9] H. Wei, Q. Shen, Y. Zhao, D.-J. Wang, D.-F. Xu, J. Cryst. Growth 250 (2003) 516–524.
[10] H. Liu, P. Lan, S. Lu, S. Wu, J. Cryst. Growth 492 (2018) 114–121.
[11] T. Zheng, H. Yi, S. Zhang, C. Wang, J. Cryst. Growth 549 (2020) 125870.
[12] A.R. Ibrahim, X. Zhang, Y. Hong, Y. Su, H. Wang, J. Li, Cryst. Growth Des. 14 (2014) 2733–2741.
[13] A.D. Trofimov, A.A. Ivanova, M.V. Zyuzin, A.S. Timin, Pharmaceutics 10 (2018) 167.
[14] B. Rugabirwa, D. Murindababisha, Y. Li, Y. Hong, Y. Su, H. Wang, J. Li, ACS Sustain. Chem. Eng. 7 (2019) 6251–6258.
[15] A.S. Schenk, B. Cantaert, Y.-Y. Kim, Y. Li, E.S. Read, M. Semsarilar, S.P. Armes, F.C. Meldrum, Chem. Mater. 26 (2014) 2703–2711.
[16] J.J. De Yoreo, P.G. Vekilov, Rev. Mineral. Geochem. 54 (2003) 57–93.
[17] R. Demichelis, A. Schuitemaker, N.A. Garcia, K.B. Koziara, M.D.L. Pierre, P. Raiteri, J.D. Gale, Annu. Rev. Mater. Res. 48 (2018) 327–352.
[18] B. Wang, Z. Pan, Z. Du, H. Cheng, F. Cheng, J. Hazard. Mater. 369 (2019) 236–243.
[19] J. Skubiszewska-Zięba, B. Charmas, H. Waniak-Nowicka, Adsorpt. Sci. Technol. 35 (2017) 668–676.
[20] X. Huang, J. Zhang, L. Zhang, Construct. Build. Mater. 411 (2024) 134603.
[21] W. Li, Y. Huang, T. Wang, M. Fang, Y. Li, J. Clean. Prod. 363 (2022) 132463.
[22] F. Zhu, L. Cui, Y. Liu, L. Zou, J. Hou, C. Li, G. Wu, R. Xu, B. Jiang, Z. Wang, Sustainability 16 (2024) 81.
[23] B. Wu, H. Wang, C. Li, Y. Gong, Y. Wang, Sustainability 15 (2023) 9629.
[24] Z. Fei, Q. Bao, X. Zheng, L. Zhang, X. Wang, Y. Wei, S. Yan, L. Ji, J. Clean. Prod. 338 (2022) 130565.
[25] F.J. Doucet, Miner. Eng. 23 (2010) 262–269.
[26] K. Cui, H. Mao, Y. Zhang, J. Wang, F. Shen, Ceram. Int. 48 (2022) 35555–35567.
[27] K. Cui, J. Wang, H. Wang, Y. Zhang, T. Fu, Steel Res. Int. 93 (2022) 2200266.
[28] Y.-N. Sheen, D.-H. Le, T.-H. Sun, Construct. Build. Mater. 101 (2015) 268–276.
[29] G. Wang, Y. Wang, Z. Gao, J. Hazard. Mater. 184 (2010) 555–560.
[30] I. Arribas, I. Vegas, J.T. San-José, J.M. Manso, Mater. Des. 63 (2014) 168–176.
[31] B. Das, S. Prakash, P.S.R. Reddy, V.N. Misra, Resour. Conserv. Recycl. 50 (2007) 40–57.
[32] H. Ding, H. Zheng, X. Liang, L. Ren, J. Clean. Prod. 244 (2020) 118953.
[33] Y. Luo, D. He, Environ. Sci. Pollut. Res. 28 (2021) 49383–49409.
[34] J.F. Young, R.L. Berger, J. Breese, J. Am. Ceram. Soc. 57 (1974) 394–397.
[35] S. Zhang, Z. Ghouleh, A. Mucci, O. Bahn, R. Provençal, Y. Shao, J. Clean. Prod. 342 (2022) 130948.
[36] E. Ren, S. Tang, C. Liu, H. Yue, C. Li, B. Liang, Greenhouse Gases: Sci. Technol. 10 (2020) 436–448.
[37] Y.-R. Yi, Y. Lin, Y.-C. Du, S.-Q. Bai, Z.-L. Ma, Y.-G. Chen, Construct. Build. Mater. 276 (2021) 122235.
[38] B.J. Zhan, D.X. Xuan, C.S. Poon, C.J. Shi, Cement Concr. Compos. 97 (2019) 78–88.
[39] E.R. Bobicki, Q. Liu, Z. Xu, H. Zeng, Energ. Combust. 38 (2012) 302–320.
[40] Z. Chen, Z. Cang, F. Yang, J. Zhang, L. Zhang, J. CO_2 Util. 54 (2021) 101738.
[41] L. Liu, M. Gan, X. Fan, Z. Sun, J. Wei, J. Li, Z. Ji, J. Environ. Chem. Eng. 11 (2023) 110655.
[42] A. Azdarpour, M. Asadullah, R. Junin, M.A. Manan, H. Hamidi, A.R.M. Daud, Energy Proc. 61 (2014) 2783–2786.
[43] T. Murakami, Y. Sugano, T. Narushima, Y. Iguchi, C. Ouchi, ISIJ Int. 51 (2011) 901–905.
[44] Y.W. Chiang, R.M. Santos, J. Elsen, B. Meesschaert, J.A. Martens, T. van Gerven, Chem. Eng. J. 249 (2014) 260–269.
[45] S. Yadav, A. Mehra, Environ. Sci. Pollut. Res. 28 (2021) 12202–12231.
[46] H. Jo, M.-G. Lee, J. Park, K.-D. Jung, Energy 120 (2017) 884–894.
[47] D. Abhilash, P. Meshram, S. Sarkar, T. Venugopalan, Miner. Metall. Process. 34 (2017) 178–182.
[48] X. Zheng, L. Ji, M. Liu, H. Zhai, K. Li, Q. He, S. Yan, Chem. Eng. J. 480 (2024) 148037.
[49] H. Tong, W. Ma, L. Wang, P. Wan, J. Hu, L. Cao, Biomaterials 25 (2014) 3923–3929.
[50] M. Mun, H. Cho, Energy Proc. 37 (2013) 6999–7005.
[51] W. Bao, H. Li, Y. Zhang, Ind. Eng. Chem. Res. 49 (2010) 2055–2063.
[52] S. Eloneva, A. Said, C.-J. Fogelholm, R. Zevenhoven, Appl. Energy 90 (2012) 329–334.
[53] M. Owais, M. Järvinen, P. Taskinen, A. Said, J. CO_2 Util. 31 (2019) 1–7.
[54] S. Kodama, T. Nishimoto, N. Yamamoto, K. Yogo, K. Yamada, Energy 33 (2008) 776–784.
[55] S. Eloneva, S. Teir, J. Salminen, C.-J. Fogelholm, R. Zevenhoven, Ind. Eng. Chem. Res. 47 (2008) 7104–7111.
[56] Y. Sun, M.-S. Yao, J.-P. Zhang, G. Yang, Chem. Eng. J. 173 (2011) 437–445.
[57] Z. Tong, G. Ma, D. Zhou, G. Yang, C. Peng, Sci. Rep. 9 (2019) 7676.
[58] S. Teir, S. Eloneva, C.-J. Fogelholm, R. Zevenhoven, Energy 32 (2007) 528–539.
[59] H. Sadeghi Ghari, A. Jalali-Arani, Appl. Clay Sci. 119 (2016) 348–357.
[60] Q. Xu, Z. Gao, D. Zhang, Q. Huang, J. Liu, B. Lu, R. Jiang, J. Mater. Civ. Eng. 36 (2024) 04023504.
[61] X. Song, Y. Tuo, Y. Liang, Z. Tang, M. Li, X. Hua, R. Yang, X. Bu, X. Luo, J. Environ. Chem. Eng. 11 (2023) 111583.
[62] J. Yao, Q. Chen, L. Zeng, W. Ding, Particuology 90 (2024) 1–9.
[63] Y. Ding, J. Zhang, B. Wang, Y. Guo, F. Xue, F. Cheng, J. Synth. Cryst. 52 (2023) 710–720 (in Chinese).
[64] B. Guo, T. Zhao, F. Sha, F. Zhang, Q. Li, J. Zhao, J. Zhang, J. CO_2 Util. 18 (2017) 23–29.
[65] T. Zhang, G. Chu, J. Lyu, Y. Cao, W. Xu, K. Ma, L. Song, H. Yue, B. Liang, Chin. J. Chem. Eng. 43 (2022) 86–98.
[66] Y. Wang, B. Ye, Z. Hong, Y. Wang, M. Liu, J. Clean. Prod. 253 (2020) 119930.
[67] L. Ma, T. Yang, Y. Wu, X. Yue, J. Yang, S. Zhang, Q. Li, J. Zhang, Kor. J. Chem. Eng. 36 (2019) 1432–1440.
[68] M. Altiner, Arab. J. Chem. 12 (2019) 531–540.
[69] S. Mao, Y. Liu, T.-A. Zhang, X. Li, Mater. Res. Express 7 (2020) 115003.
[70] X. Wang, M.M. Maroto-Valer, Fuel 90 (2011) 1229–1237.
[71] J. Hu, W. Liu, L. Wang, Q. Liu, F. Chen, H. Yue, B. Liang, L. Lü, Y. Wang, G. Zhang, C. Li, J. Energy Chem. 26 (2017) 927–935.
[72] X. Zheng, J. Liu, Y. Wei, K. Li, H. Yu, X. Wang, L. Ji, S. Yan, Chem. Eng. J. 440 (2022) 135900.
[73] Y.I. Svenskaya, H. Fattah, O.A. Inozemtseva, A.G. Ivanova, S.N. Shtykov, D.A. Gorin, B.V. Parakhonskiy, Cryst. Growth Des. 18 (2018) 331–337.
[74] N. Cheng, M.F. Zhou, P.Y. Chen, C.Z. Li, H.B. Jiang, L. Zhang, Process Eng. 17 (2017) 412–419 (in Chinese).
[75] J.A.M. van der Houwen, G. Cressey, B.A. Cressey, E. Valsami-Jones, J. Cryst. Growth 249 (2003) 572–583.
[76] S.F. Chen, S.H. Yu, J. Jiang, F. Li, Y. Liu, Chem. Mater. 18 (2006) 115–122.
[77] K. Song, Y.-N. Jang, W. Kim, M.G. Lee, D. Shin, J.-H. Bang, C.W. Jeon, S.C. Chae, Chem. Eng. J. 213 (2012) 251–258.
[78] D. Konopacka-Łyskawa, B. Kościelska, M. Łapiński, J. Occup. Med. 71 (2019) 1041–1048.

[79] Z. Wang, L. Cui, Y. Liu, J. Hou, H. Li, L. Zou, F. Zhu, Front. Environ. Sci. Eng. 18 (2023) 12.
[80] D. Konopacka-Łyskawa, B. Kościelska, J. Karczewski, A. Gołąbiewska, Mater. Chem. Phys. 193 (2017) 13–18.
[81] W. Li, G. Chen, F. Zhang, J. Sun, Sep. Purif. Technol. 317 (2023) 123932.
[82] B. Wang, Z. Pan, H. Cheng, Z. Zhang, F. Cheng, J. Clean. Prod. 302 (2021) 126930.
[83] M. Altıner, J. Int, Coal Prep. Util. 39 (2018) 1–19.
[84] W.Y. Tan, W.H. Fan, H.Y. Lin, Z.X. Zhang, Y.K. Zhu, Waste Manag. Res. 35 (2017) 1296–1301.
[85] M.G. Lee, Y.N. Jang, K.W. Ryu, W. Kim, J.-H. Bang, Energy 47 (2012) 370–377.
[86] X. Liu, B. Wang, Z. Zhang, Z. Pan, H. Cheng, F. Cheng, Environ. Chem. Lett. 20 (2022) 2261–2269.
[87] A. Azdarpour, M. Asadullah, R. Junin, E. Mohammadian, H. Hamidi, A.R.M. Daud, M. Manan, Fuel Process. Technol. 130 (2015) 12–19.
[88] K.-M. Choi, K. Kuroda, Cryst. Growth Des. 12 (2012) 887–893.
[89] H. Zhao, H. Li, W. Bao, C. Wang, S. Li, W. Lin, J. CO_2 Util. 11 (2015) 10–19.
[90] A. Azdarpour, M. Asadullah, R. Junin, M. Manan, H. Hamidi, E. Mohammadian, Fuel Process. Technol. 126 (2014) 429–434.
[91] M.G. Lee, K.W. Ryu, S.C. Chae, Y.N. Jang, Environ. Technol. 36 (2015) 106–114.
[92] M.-G. Lee, D. Kang, H. Jo, J. Park, J. Mater. Cycles. Waste 18 (2016) 407–412.
[93] K. Song, Y.-N. Jang, W. Kim, M.G. Lee, D. Shin, J.-H. Bang, C.W. Jeon, S.C. Chae, Energy 65 (2014) 527–532.
[94] K. Song, W. Kim, J.-H. Bang, S. Park, C.W. Jeon, Mater. Des. 83 (2015) 308–313.
[95] W. Ding, Q. Chen, H. Sun, T. Peng, J. CO_2 Util. 34 (2019) 507–515.
[96] H. Cheng, X. Wang, B. Wang, J. Zhao, Y. Liu, F. Cheng, J. Cryst. Growth 469 (2017) 97–105.
[97] J. Luo, F. Kong, X. Ma, Cryst. Growth Des. 16 (2016) 728–736.
[98] Y. Lai, L. Chen, W. Bao, Y. Ren, Y. Gao, Y. Yin, Y. Zhao, Cryst. Growth Des. 15 (2015) 1194–1200.
[99] M. Altiner, S. Top, B. Kaymakoğlu, İ.Y. Seçkin, H. Vapur, J. CO_2 Util. 29 (2019) 117–125.
[100] K. Song, W. Kim, S. Park, J.-H. Bang, C.W. Jeon, J.-W. Ahn, Chem. Eng. J. 301 (2016) 51–57.
[101] B. Wang, Z. Pan, H. Cheng, Y. Guan, Z. Zhang, F. Cheng, Environ. Chem. Lett. 18 (2020) 1369–1377.
[102] A. Lachehab, O. Mertah, A. Kherbeche, H. Hassoune, Mater. Sci. Energy Technol. 3 (2020) 611–625.
[103] D. Yelatontsev, Production Reserves 3 (2021) 10–13.
[104] M. Contreras, R. Pérez-López, M.J. Gázquez, V. Morales-Flórez, A. Santos, L. Esquivias, J.P. Bolívar, Waste Manage. (Tucson, Ariz.) 45 (2015) 412–419.
[105] L. Ji, H. Yu, K. Li, B. Yu, M. Grigore, Q. Yang, X. Wang, Z. Chen, M. Zeng, S. Zhao, Appl. Energy 225 (2018) 356–366.
[106] B. Yu, H. Yu, K. Li, L. Ji, Q. Yang, X. Wang, Z. Chen, M. Megharaj, Environ. Sci. Technol. 52 (2018) 13629–13637.
[107] G. Gadikota, Nat. Rev. Chem. 4 (2020) 78–89.
[108] M. Liu, G. Gadikota, Energy Fuels 33 (2019) 1722–1733.
[109] L. Ji, X. Zheng, L. Zhang, L. Feng, K. Li, H. Yu, S. Yan, Chem. Eng. J. 430 (2022) 133118.
[110] H.-J. Ho, A. Iizuka, E. Shibata, J. Environ. Manag. 288 (2021) 112411.
[111] T.K. Choo, B. Etschmann, C. Selomulya, L. Zhang, Energy Fuels 30 (2016) 3269–3280.
[112] T. Hosseini, N. Haque, C. Selomulya, L. Zhang, Appl. Energy 175 (2016) 54–68.
[113] H.-J. Ho, A. Iizuka, E. Shibata, T.V. Ojumu, J. Environ. Chem. Eng. 10 (2022) 108269.
[114] L. He, D. Yu, W. Lv, J. Wu, M. Xu, Ind. Eng. Chem. Res. 52 (2013) 15138–15145.
[115] X. Wang, M.M. Maroto-Valer, Energy 51 (2013) 431–438.
[116] X. Zheng, J. Liu, Y. Wang, Y. Wang, L. Ji, S. Yan, Chem. Eng. J. 459 (2023) 141536.
[117] A. Kai, K. Fujikawa, T. Miki, Jpn. Appl. Phys. 41 (2002) 439.
[118] R. Marin Rivera, T. Van Gerven, J. CO_2 Util. 41 (2020) 101241.
[119] D. Fernandes, W. Conway, X. Wang, R. Burns, G. Lawrance, M. Maeder, G. Puxty, J. Chem. Thermodyn. 51 (2012) 97–102.
[120] L. Ji, H. Yu, B. Yu, K. Jiang, M. Grigore, X. Wang, S. Zhao, K. Li, Chem. Eng. J. 352 (2018) 151–162.
[121] Q. Yang, G. Puxty, S. James, M. Bown, P. Feron, W. Conway, Energy Fuels 30 (2016) 7503–7510.
[122] N. Wada, N. Horiuchi, M. Nakamura, K. Nozaki, A. Nagai, K. Yamashita, Cryst. Growth Des. 18 (2018) 872–878.
[123] Y. Huang, X. Zheng, Y. Wei, Q. He, S. Yan, L. Ji, Chem. Eng. J. 450 (2022) 138121.
[124] D. Madhav, B. Buffel, F. Desplentere, P. Moldenaers, V. Vandeginste, Fuel 345 (2023) 128157.
[125] K. Chen, S. Han, F. Meng, L. Lin, J. Li, Y. Gao, W. Qin, E. Hu, J. Jiang, Chem. Eng. J. 481 (2024) 148392.
[126] X. Shao, B. Qin, Q. Shi, Y. Yang, Z. Ma, Y. Xu, M. Hao, Z. Jiang, W. Jiang, Fuel 334 (2023) 126378.
[127] L. Ji, H. Yu, R. Zhang, D. French, M. Grigore, B. Yu, X. Wang, J. Yu, S. Zhao, Fuel Process. Technol. 188 (2019) 79–88.
[128] G. Montes-Hernandez, R. Pérez-López, F. Renard, J.M. Nieto, L. Charlet, J. Hazard. Mater. 161 (2009) 1347–1354.
[129] Y. Sun, V. Parikh, L. Zhang, J. Hazard. Mater. 209–210 (2012) 458–466.
[130] K.R. Senadeera, T.K. Jayasinghe, P.M. Jayasundara, G. Nanayakkara, M. Rathnayake, MERCON 2020: 6th International Multidisciplinary Moratuwa Engineering Research Conference, Mercon, 2020, pp. 119–123.
[131] Y. Zhong, T. Shi, Q. Chen, X. Yang, D. Xu, Z. Zhang, X. Wang, B. Zhong, Chin. J. Chem. Eng. 28 (2020) 208–215.
[132] D. Gebauer, Minerals 8 (2018) 179.
[133] A. Said, T. Laukkanen, M. Järvinen, Appl. Energy 177 (2016) 602–611.
[134] A. Iizuka, T. Sasaki, M. Honma, H. Yoshida, Y. Hayakawa, Y. Yanagisawa, A. Yamasaki, Chem. Eng. Commun. 204 (2017) 79–85.
[135] S. Park, Y. Ahn, S. Lee, J. Choi, J. Hazard. Mater. 403 (2021) 123862.
[136] H. Xie, H. Yue, J. Zhu, B. Liang, C. Li, Y. Wang, L. Xie, X. Zhou, Engineering 1 (2015) 150–157.
[137] K. Pan, H. Li, C. Wang, W. Bao, K. Huang, D. Liao, Adv. Mater. Res. 878 (2014) 244–253.
[138] China Powder Network, Breakthrough in Carbonation Utilization Technology of Industrial Solid Waste in China (2024). http://www.cnpowder.com.cn/news/32015.html. (Accessed 16 July 2024).
[139] A. Sanna, M. Uibu, G. Caramanna, R. Kuusik, M. Maroto-Valer, Chem. Soc. Rev. 43 (2014) 8049–8080.
[140] S.J. Gerdemann, W.K. O'Connor, D.C. Dahlin, L.R. Penner, H. Rush, Environ. Sci. Technol. 41 (2007) 2587–2593.
[141] R.D. Balucan, B.Z. Dlugogorski, E.M. Kennedy, I.V. Belova, G.E. Murch, Int. J. Greenh. Gas Control 17 (2013) 225–239.
[142] A. Fedoročková, M. Hreus, P. Raschman, G. Sučik, Miner. Eng. 32 (2012) 1–4.
[143] J. Li, M. Hitch, Int. Biodeterior. Biodegrad. 128 (2018) 63–71.
[144] J.K. Stolaroff, G.V. Lowry, D.W. Keith, Energy Convers. Manag. 46 (2005) 687–699.
[145] W.J.J. Huijgen, R.N.J. Comans, G.J. Witkamp, Energy Convers. Manag. 48 (2007) 1923–1935.
[146] S.Y. Pan, A. Chiang, E.E. Chang, Y.P. Lin, H. Kim, P.C. Chiang, Aerosol Air Qual. Res. 15 (2015) 1072–1091.
[147] S. Teir, R. Kuusik, C.J. Fogelholm, R. Zevehoven, Int. J. Miner. Process. 85 (2007) 1–15.
[148] S. Teir, S. Eloneva, C.J. Fogelholm, R. Zevehoven, Appl. Energy 86 (2009) 214–218.
[149] O. Rahmani, M. Tyrer, R. Junin, RSC Adv. 4 (2014) 45548–45557.